

Impact and evaluation of potential implications of coastal plains on soil greenhouse gas emissions

Insights from the Sibari Coastal Plain (Calabria, Southern Italy)

Apollaro, C.; Vespasiano, G.; Fuoco, I.; Taussi, M.; De Rosa, R.; La Russa, M. F.; Guido, A.; Di Curzio, D.; Renzulli, A.; Russo, L.

DOI

[10.1016/j.scitotenv.2025.178611](https://doi.org/10.1016/j.scitotenv.2025.178611)

Publication date

2025

Document Version

Final published version

Published in

Science of the Total Environment

Citation (APA)

Apollaro, C., Vespasiano, G., Fuoco, I., Taussi, M., De Rosa, R., La Russa, M. F., Guido, A., Di Curzio, D., Renzulli, A., Russo, L., Ciniglia, F., D'Amico, F., Cipriani, M., Maruca, G., Virgili, G., & Bloise, A. (2025). Impact and evaluation of potential implications of coastal plains on soil greenhouse gas emissions: Insights from the Sibari Coastal Plain (Calabria, Southern Italy). *Science of the Total Environment*, 964, Article 178611. <https://doi.org/10.1016/j.scitotenv.2025.178611>

Important note

To cite this publication, please use the final published version (if applicable).
Please check the document version above.

Copyright

Other than for strictly personal use, it is not permitted to download, forward or distribute the text or part of it, without the consent of the author(s) and/or copyright holder(s), unless the work is under an open content license such as Creative Commons.

Takedown policy

Please contact us and provide details if you believe this document breaches copyrights.
We will remove access to the work immediately and investigate your claim.



Impact and evaluation of potential implications of coastal plains on soil greenhouse gas emissions: Insights from the Sibari Coastal Plain (Calabria, Southern Italy)

C. Apollaro^a, G. Vespasiano^{a,*}, I. Fuoco^b, M. Taussi^c, R. De Rosa^a, M.F. La Russa^a, A. Guido^a, D. Di Curzio^d, A. Renzulli^c, L. Russo^a, F. Ciniglia^a, F. D'Amico^{a,e}, M. Cipriani^a, G. Maruca^a, G. Virgili^f, A. Bloise^a

^a Department of Biology, Ecology and Earth Sciences (DIBEST), University of Calabria, Ponte Bucci street, cube 15B, 87036 Rende, Italy

^b National Research Council of Italy - Institute on Membrane Technology (ITM-CNR), P. Bucci street, cube 17/C-87036, Arcavacata di Rende, Italy

^c Department of Pure and Applied Sciences, University of Urbino Carlo Bo, Ca' Le Suore street, 2/4, 61029 Urbino, Italy

^d Department of Water Management, Delft University of Technology, Stevinweg 1, 2628, CN, Delft, Netherlands

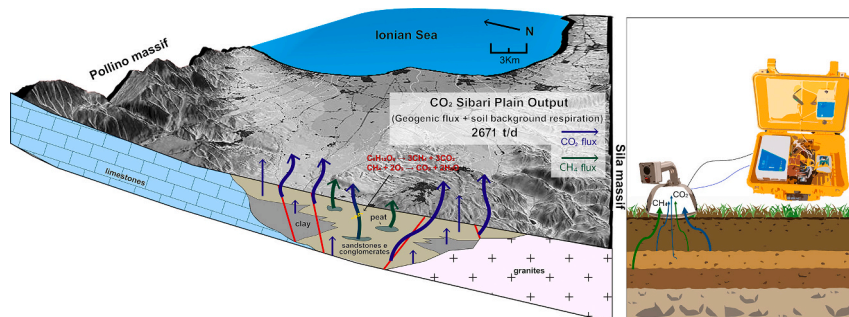
^e National Research Council of Italy - Institute of Atmospheric Sciences and Climate (ISAC-CNR), Area Industriale Comp. 15, I-88046 Lamezia Terme, Italy

^f THEAREN SRL Strada di Settimo 266, 10156 Torino, (TO), Italy

HIGHLIGHTS

- A better understanding of the relationship between geological settings and GHGs emitted from soils
- Elaboration with statistical and geostatistical methods to separate different CO₂ flux populations
- Estimation of total GHGs efflux output in a coastal plain
- Comparison of normalized fluxes with volcanic and non-volcanic areas

GRAPHICAL ABSTRACT



ARTICLE INFO

Editor: Jay Gan

Keywords:

Greenhouse gas emissions
CO₂
CH₄
Accumulation chamber
Gas emission and environmental implication
Coastal plains
Sibari plain

ABSTRACT

The work aims to estimate natural greenhouse gas emissions from soils in the Sibari Coastal Plain (Southern Italy), to understand (i) the contribution in terms of the total amount of CO₂ and CH₄ emitted in non-volcanic areas, (ii) the relationship among emitted gas, land use, organic matter and tectonic structures, and (iii) their potential environmental implications. Data were elaborated with statistical and geostatistical methods to separate the different populations and obtain prediction and probability maps. Methane fluxes had values consistently below the detection limit ($0.032 \text{ g} \cdot \text{m}^{-2} \cdot \text{d}^{-1}$) except for three measurement points randomly distributed along the plain. Statistical and geostatistical methods allowed to discriminate three main CO₂ flux populations: (i) high-flux population (Pop. B - mean value of $63.65 \text{ g} \cdot \text{m}^{-2} \cdot \text{d}^{-1}$), located near the mouth of the Crati River and related to the massive presence of buried organic matter in the form of peat; (ii) medium-flux population (Pop. A2 - mean value of $8.37 \text{ g} \cdot \text{m}^{-2} \cdot \text{d}^{-1}$) which is the result of soil respiration, and (iii) low-flux population

* Corresponding author.

E-mail address: giovanni.vespasiano@unical.it (G. Vespasiano).

<https://doi.org/10.1016/j.scitotenv.2025.178611>

Received 9 August 2024; Received in revised form 19 January 2025; Accepted 20 January 2025

Available online 24 January 2025

0048-9697/© 2025 The Authors. Published by Elsevier B.V. This is an open access article under the CC BY license (<http://creativecommons.org/licenses/by/4.0/>).

(Pop. A1 - mean value of $1.85 \text{ g} \cdot \text{m}^{-2} \cdot \text{d}^{-1}$) due to areas where low permeability or increases in saturated aquifer thickness may control the overall flux.

In the study area, a total CO_2 emission of about $2671 \text{ t} \cdot \text{d}^{-1}$ was calculated, which, if compared to the average total flux expected for simple soil respiration ($1284 \text{ t} \cdot \text{d}^{-1}$), represents a non-negligible value in the total Carbon balance. Finally, the comparison with representative normalized fluxes from volcanic and non-volcanic areas confirms the critical role of coastal plains in total atmospheric CO_2 emissions. The proposed approach can be applied to areas with comparable or different geological and climatic settings to trace their contribution in terms of greenhouse gas release to the atmosphere.

1. Introduction

In the past decades, one of the main goals of the scientific community was to discriminate different sources of greenhouse gas (GHG) emissions (e.g., CO_2 , CH_4 , NO_x , and N_2O), quantify their individual contributions and identify increasingly efficient approaches to reduce their total emission outputs. The concentration of CO_2 in the atmosphere increased in the last three centuries. In 1750, which is usually considered representative of pre-industrial levels, the concentration in the atmosphere was about 278 ppm (Nefel et al., 1985), whereas a value of about 423 ppm is currently reported (GML – National Oceanic and Atmospheric Administration, 2024). One of the main issues related to atmospheric CO_2 is its prolonged residence time (according to estimates, extra anthropogenic emissions may require up to 100,000 years to be removed by natural processes) and its capacity to affect the climate via radiative forcing (e.g., Ma et al., 2021; Montzka, 2023). In addition, CO_2 increases in natural systems (e.g., hydrosphere) enhance water-rock interaction processes promoting the release of constituents (e.g., Fe, Zn, Cr and Sn), which could be harmful to human health (Apollaro et al., 2007a, 2007b, 2019, 2023; Kokh et al., 2017). The concentration of CH_4 in the atmosphere has also increased in the last three centuries, and its impacts on solar radiative forcing have also been characterized (Byrom and Shine, 2022). Anthropogenic emissions such as combustion processes and livestock are deemed responsible for multi-year upward trends in atmospheric methane (Skeie et al., 2023). CH_4 in the atmosphere reached 1866.58 ± 0.60 ppb in 2019 (Lan et al., 2024), and 1911.9 ppb in 2022 (Blunden et al., 2023). These gases are the result of both anthropogenic activities and natural processes. CO_2 and CH_4 are frequently subject to continuous atmospheric measurements to discriminate anthropogenic emissions from natural outputs (Rella et al., 2015; Dickinson et al., 2017).

In the natural domain, there are two main categories of sources: biological (e.g., metabolic activities of organisms and taphonomic processes of decaying organic matter) and abiotic (e.g., volcanic and/or hydrothermal activities and metamorphic processes involving carbonates species) which in turn can be the cause of diffused or punctual GHGs emissions. Classical diffusion mechanisms include soil emissions associated to both biological and abiotic activities. The biological one is mainly related to soil respiration (Rs), an essential component of Earth's ecosystem functioning and a fundamental process in the exchange of CO_2 between land and the atmosphere (He et al., 2024). The amount of GHGs emitted from soils can be extremely variable, and the study of the spatial distribution of these emissions allows us to trace the amount of gas emitted per specific surface area, identifying possible correlations with local structures, lithologies and other factors. For instance, this approach was used in the past for different purposes: oil research (Etioppe et al., 2009), monitoring of active tectonic structures (Barnes et al., 1978; Irwin and Barnes, 1980; Yuce et al., 2017; Liu et al., 2023), investigation of buried fault systems (Guerra and Lombardi, 2001; Baubron et al., 2002; Fu et al., 2005; Lombardi and Voltattorni, 2010), studies of volcanic and geothermal areas (Corazza et al., 1993; Chiodini et al., 1998; Phuong et al., 2012; Carapezza et al., 2015; Cardellini et al., 2017; Randazzo et al., 2022; Taussi et al., 2021, 2023; Tardani et al., 2024), and even in the assessment of landfill emissions (Battaglini et al., 2013; Li et al., 2020). All these works focused on the most common

GHGs emitted from soils: CO_2 , and/or CH_4 . One of the most popular methods to measure soil gas fluxes is the accumulation chamber, an instrument that allows the measurement of soil fluxes of different gaseous species, presenting several advantages over other methods (Tonani and Miele, 1991; Chiodini et al., 1998; Tregoures et al., 1999). Although the chamber method is mainly applied in studying of volcanic or geothermal areas (Project PRIN, 2022 - PNRR), and agricultural soils, it is also helpful in investigating CO_2 and CH_4 fluxes emitted from the soil in non-volcanic regions such as coastal plains. Coastal plains have generally been underestimated in their contribution to GHGs emissions. However, geological complexities such as a considerable amount of buried organic matter (e.g., peats) often promote anomalous and diffuse emissions of GHGs that cannot be overlooked in the total Carbon balance. Peat results from decomposition of organic substances, vegetable in origin, in conditions that match anoxic specifications (e.g., Harriss et al., 1985; Lyons and Alpern, 1989). Peatlands are a subcategory of wetlands that release CH_4 and CO_2 naturally (e.g., Aselmann and Crutzen, 1990; Martikainen et al., 1994). The methane production rates show several degrees of variability, depending on factors such as the depth of peat and water tables, and the type of soil and vegetation involved (Frenzel and Karofeld, 2000; Whalen and Reeburgh, 2000). Temperature has also been confirmed to affect methane emissions (Waddington and Day, 2007).

In Coastal Plains, geogenic CO_2 can have different origins, related to mantle degassing, carbonate metamorphism, carbonate dissolution, or organic matter oxidation (Irwin and Barnes, 1980; Baubron et al., 2002; Italiano et al., 2009; Caracausi et al., 2015). The Calabria region has ≈ 800 km of coastline along which wide coastal plains develop, such as the plains of Lamezia Terme (Sant'Eufemia plain) (Vespasiano et al., 2016; Vespasiano et al., 2023a), Crotona (Cannata et al., 2016; Vespasiano et al., 2021), Gioia Tauro (Cianflone et al., 2021, 2022; Vespasiano et al., 2023b), Reggio Calabria (Vespasiano et al., 2018), and Sibari (Cianflone et al., 2018; Vespasiano et al., 2015a, 2015b, 2019, 2023c). These plains are characterized by lithological and structural frameworks that may promote the formation of anomalous fluxes due to shallow and deep processes.

To investigate this aspect, this work aims to assess for the first time the contribution, in terms of GHGs emissions, of the Sibari Coastal Plain (Calabria – South Italy). These findings are aimed to integrate current knowledge on global GHGs budgets and balances (e.g., Keeling, 1958; Pales and Keeling, 1965; Saunio et al., 2016, 2017, 2020), as well as continuous atmospheric measurements performed at local Mediterranean WMO/GAW (World Meteorological Organization – Global Atmosphere Watch) observation sites (e.g., Cristofanelli et al., 2017). This site was selected for its lithological, stratigraphic, and structural settings. In detail, the main scope includes: (i) identifying anomalous fluxes in terms of CO_2 and CH_4 along a selected portion of the Sibari Plain; (ii) correlating fluxes to the lithological and structural evidence of the area; (iii) quantifying source-specific fluxes and compare them with fluxes recognized in geothermal volcanic and non-volcanic areas. This study, and others following the protocol here discussed, can contribute to a better understanding of the amount and distribution of natural CO_2 and CH_4 emissions, and their contribution to the increasing GHGs concentrations in the atmosphere, considering that approximately 10 % of the atmosphere's carbon passes through soils each year (Raich and

Tufekciogul, 2000).

2. Geological and hydrogeological setting

The Sibari Coastal Plain (SCP) is located in the northeastern area of the Calabrian-Peloritan Orogen (CPO - [Cirrincione et al., 2015](#)), between the Sila Massif and the Pollino Chain ([Van Dijk et al., 2000](#)), in the last portion of the Crati Valley ([Fig. 1a, b](#)), which represents the most extended Calabrian plain (470 km²). In the 1930s, the SCP was reclaimed and made cultivable (mainly in rice paddies and orange groves). This led to a diffused agricultural activity which, along with tourism, represents the main local economic resource.

From a geological point of view, in the northern part of the SCP, the carbonatic-dolomitic bedrock (Pollino chain) is progressively covered by the Torrente Straface unit (Pliocene), the Pleistocene sandy marine deposits, and the Holocene successions ([Apollaro et al., 2020](#); [Vespasiano et al., 2015c](#) and reference therein). Here, the Satanasso and Saraceno rivers represent the current primary sediment sources, generating important alluvial fans. In the central part of the plain, a thick evaporitic succession (which overlays the basement) is covered by Pliocene and Quaternary sediments. The sedimentary succession and the morphological setting are the result of processes such as the migration of Crati's delta (7 km over the last 6 ka; [Cianflone et al., 2013](#)), the Messinian salinity crisis ([Cipriani et al., 2021, 2023, 2024](#); [Perri et al., 2023, 2024](#)), and the subsidence of the area ([Cianflone et al., 2018](#)). Finally, in the southern part, the crystalline basement (Sila Massif) is covered by

Miocenic conglomerates and sandstones, followed upward by Pliocenic clays and Pleistocenic conglomerates and sandstone. The main sources of sediment in this area (that belong to the Corigliano basin) are the Crati and Trionto rivers ([ViDEPI; Cianflone et al., 2018; Vespasiano et al., 2019](#)).

Several tectonic alignments border the SCP. The main regional fault system is represented by the "Sanginetto Line" ([Fig. 1b](#)), a WSW-ENE high-angle faults system which, together with its trans-tensional kinematics, marks the contact between the Apennines and Calabria terranes and affects the geodynamics of the area during the Quaternary ([Tansi et al., 2007](#)). The "Corigliano-Rossano fault" (WNW-ESE), instead, shows strike-slip (left-lateral) kinematics and separates the plain from the Sila massif ([Lanzafame and Tortorici, 1981](#)). The internal tectonic elements are mainly represented by two main NE-SW faults, the Crati and Timparelle Faults ([Fig. 1](#)), also reported in the National Catalogue of Capable Faults ([Comerci et al., 2013](#)). These systems have no surface evidence due to recent sedimentary cover. In the past years, several authors ([Cinti et al., 2015, 2024](#)) have reported evidence of another NE-SW extensional fault, the so-called "Sibari Fault Zone" (SFZ). The authors studied the relations between records of human settlements in the Sibari Plain (the old Sibarys, which dates to the ancient Greek colonization of Calabria), earthquakes, and faults. They found some co-seismic evidence (such as shifted or rotated walls) which allowed the identification of the last fault activity during the II and IX centuries A.D. and thus deem the NE-SW faults active and capable of generating earthquakes ([Comerci et al., 2013; Cianflone et al., 2018](#)).

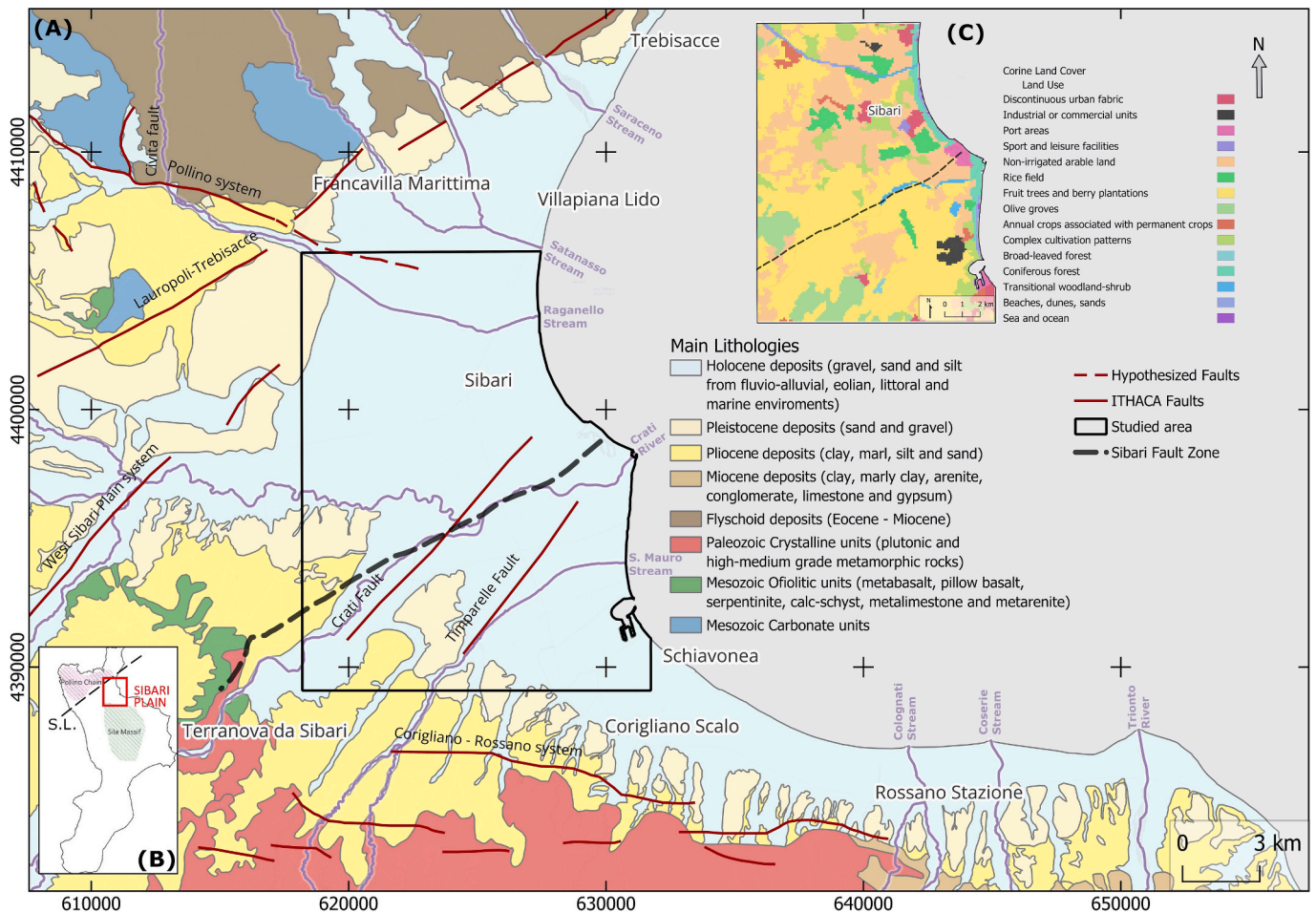


Fig. 1. (a) Simplified large-scale geological map of the Sibari Plain area. The polygonal-shaped area corresponds to the studied area. The red-coloured units correspond to the Sila crystalline terrains, while the blue-coloured, in the northernmost portion, correspond to carbonates and dolomites of the Pollino massif. (b) Regional map showing the main massifs (Sila and Pollino) which characterize the northern portion of Calabria region with location of the studied area. S.L. corresponds to "Sanginetto Line". (c) Land use map of the Sibari Coastal Plain ([Corine Land Cover, 2019](#)).

In the SCP area, an important subsidence process was recently recognized. As reported by Cianflone et al. (2015), the process is related to different causes, such as the lithostatic weight of Quaternary successions, intensive groundwater pumping, massive presence of buildings, and anthropic activities. The presence of faults results in different rates of subsidence in the area that create the accommodation space for the accumulation of sediment and organic matter (e.g., peat) (Cianflone et al., 2018).

From a hydrogeological point of view, two main aquifers have been identified in the Sibari Plain (Vespasiano et al., 2019): a shallow phreatic aquifer (20/30 m b.g.l.) and a deep confined aquifer (50/60 m b.g.l.), separated by a clayey-silty layer. The deep artesian aquifer shows, in proximity to the Crati mouth, high salinity (up to 4500 $\mu\text{S}/\text{cm}$) with Cl concentrations sporadically exceeding 2000 ppm (Vespasiano et al., 2019). Several authors relate these anomalies to the high residence time of water (Tazioli, 1986) or to mixing processes with seawater and/or upwelling of brackish waters via faults (Guerricchio et al., 1976; Polemio and Luise, 2007; Vespasiano et al., 2015a; Vespasiano et al., 2019).

The land use of the area is currently mainly devoted to agricultural crops consisting of fruit trees (primarily peaches and citrus) and rice fields interrupted occasionally by urbanized and industrialized areas (Fig. 1c; Corine Land Cover, 2019). In terms of permeability, the innermost portions, where Pliocene clays outcrop, show the lowest values (Cianflone et al., 2018), whereas the coastal sectors characterized by alluvial fans and coarse Pleistocene and Holocene deposits, show higher permeabilities.

3. Methods

The gas flux in the soil was measured with an accumulation chamber (Chiodini et al., 1998; Pavelka et al., 2018). This device was proposed in 1927 by Henrik Ludengård to study the evolution of carbon dioxide in the soil and its relationship with crop growth. There are two main classes of accumulation chambers: static stationary and static non-stationary (SNPA, 2018). Chambers of the first type are placed and left in the soil until the analyte concentration reaches a stationary level. The non-stationary static chambers are placed on the ground and left in measurement only for the time span necessary to detect the concentration gradient over time of each analyte. This parameter allows the measurement of the emission flux of a given gas species (Chiodini et al., 1998).

The system used in this work, manufactured by Thearen Ltd., uses a non-stationary static accumulation chamber. The gas mixture in the chamber is sent, via a small diaphragm pump, to analyzers that determine the concentration of CO_2 , H_2O , and CH_4 and then re-injected into the chamber. The accumulation chamber is equipped with a vent to ensure that the pressure inside the chamber is in equilibrium with the atmosphere.

Carbon dioxide and water vapour are analysed by an NDIR technology (Non-Dispersive Infrared Adsorption - Dinh et al., 2016) analyzer based on Lambert-Beer law; the analyzer, model LI-850 by LICOR, uses a black body as the IR source and a 50 mm long absorption cell.

The analysis of methane is entrusted to a TDLA analyzer (Tunable Diode Laser Infrared Adsorption) which is still based on Lambert-Beer

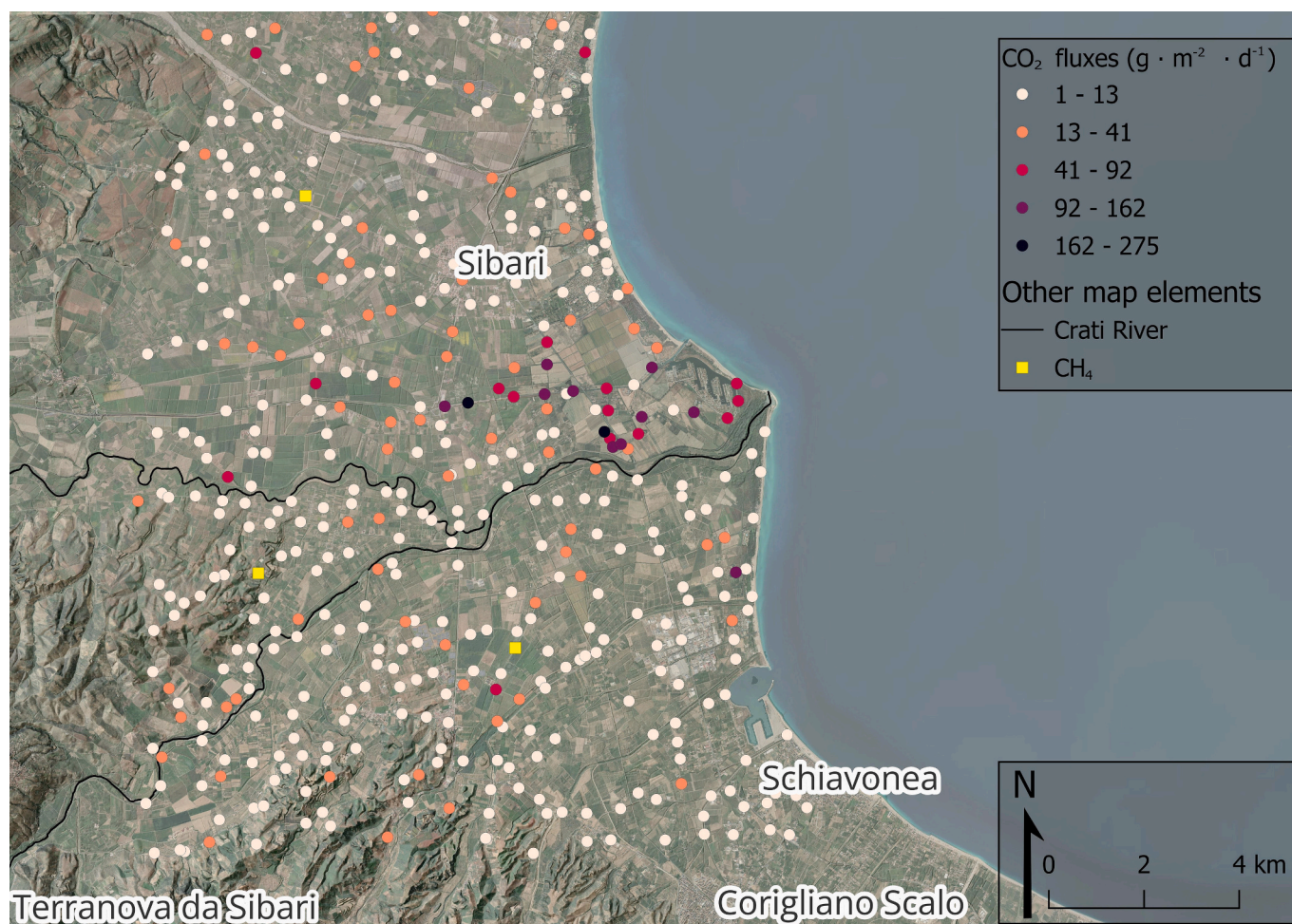


Fig. 2. Distribution of the CO_2 flux measurement points in the study area with the related values ($\text{g} \cdot \text{m}^{-2} \cdot \text{d}^{-1}$). The three yellow points represent the only samples with a CH_4 flux value above the detection limit.

law but uses a multi-pass cell with a length equivalent to a few meters as the absorption cell and a tunable laser diode as the IR source.

The instrument has the following detection limits: 0.18 to 44,000 g • m⁻² • d⁻¹ (0.004–1000 mol • m⁻² • d⁻¹) for CO₂; 0.032 to 16,000 g • m⁻² • d⁻¹ (0.002–1000 mol • m⁻² • d⁻¹) for CH₄.

To obtain a representative dataset of CO₂ and CH₄ soil emissions, 459 flux measurements were conducted along the study area (197 km²) with a sample grid of about 500 m (Fig. 2). Field activities were conducted between July and September 2023, in a period characterized by low rainfall and relatively constant temperatures/pressures. All surveys were conducted during the day. For each point, the following parameters have been defined: (i) coordinates; (ii) time of measure (UTC); (iii) atmospheric pressure and temperature; (iv) soil flux of CO₂, CH₄. For each sampling day, a few measurement points from the previous day were repeated to assess any discordance in terms of flux and atmospheric pressure.

Acquired measurements were initially cleaned by removing all negative values. Subsequently, they were processed using statistical and geostatistical techniques to provide a better understanding of soil GHGs emissions. The dataset included values (n. 7) below the limit of detection (LOD). These were excluded for the subsequent processing. The Graphical Statistical Approach (GSA) partitioning method proposed by Sinclair (1974) was applied to identify overlapping populations in the dataset. Inflection points on cumulative probability plots can discriminate the distributions due to two or more populations, considering that, in cumulative probability plots, the values of a single normally or lognormally distributed population should be aligned. In contrast, the overlapping of two or more populations will appear as a curved line with one or more inflexion points representing population thresholds (Sinclair, 1974; Panno et al., 2006). Once the thresholds are identified, populations can be separated. Subsequently, the natural background levels (NBLs) were estimated. Generally, NBLs are defined as a percentile of the dataset distribution, between the 90th and 97.7th percentiles, according to available data quality (Müller et al., 2006). In this study, by using the software ProUCL v. 5.1 (Singh and Maichle, 2015), the NBLs of CO₂ fluxes were set at the 95th percentile. Finally, the total amount of CO₂ emitted from the Sibari coastal plain and the normalized specific flux (total emission / extent of the study area expressed in km²) for each population were estimated. Specific fluxes were compared with those estimated in areas characterized by different geological contexts. The estimation of the total amount of CO₂ has been carried out by applying the Sichel's t-estimator (David, 1977). The estimated CO₂ emission rate was obtained by multiplying the area of the measured site, the average CO₂ flux value, and the proportion of each population recognized by the GSA (Elfo et al., 2016). The uncertainty of each population's CO₂ output was calculated using the central 95 % confidence intervals.

3.1. Geostatistical analysis

The interpolated maps of the soil CO₂ flux distributions were created through sequential Gaussian simulations (sGs) using the geostatistical tools provided by the ESRI ArcGIS® 10.8.2 software. The sGs algorithm was introduced by Deutsch and Journel (1992) and applied in a high number of studies (e.g., Cardellini et al., 2003; Fridriksson et al., 2006; Jácóme-Paz et al., 2019; Jentsch et al., 2020). This methodology permits to avoid the smoothing of extreme values while preserving spatial variations. A total of 100 realizations were performed for the sGs based on a simple kriging model, which was previously implemented.

There are some similarities between simple kriging and linear regression methods. From a mathematical point of view, simple kriging (often referred to as "BLUE": Best Linear Unbiased Estimate) use the following formula (Li et al., 2009):

$$Z_{SK}^*(S_0) = m + \sum_{i=1}^n \lambda_i \cdot (Z(S_i) - m) \quad (1)$$

In the case of SK, the target variable $Z_{SK}^*(S_0)$ was estimated at each

unsampled location (S_0). This method relies on an assigned weight (λ_i) which is independent of data values. It is also based on the mean (m) of the measured values $Z(s)$, a variable that must be known to use SK. Simple kriging is usually used when evaluated phenomena do not exhibit a trend (because of stationary assumption), but in some cases, simple kriging may be used under a local stationarity assumption. Another characteristic of simple kriging is that it minimizes squared error estimation (Ma and Zhang, 2019). As Cardellini et al. (2003) reported, SK is an optimal solution to estimate the mean and variance for the sGs method.

The sGs procedure requires a Gaussian distribution of data. Therefore, all data were log-normal transformed to correct data distribution before the generation of omnidirectional variograms (Table 1S). The variogram model is used to calculate the lambda weights in the BLUE estimator. A log-normal transformation has been used, and its effectiveness was evaluated by comparing the statistical distributions before and after the transformation and through probability-plots (Fig. 1S). Skewness values were additionally included to measure the symmetry of statistical distribution, which is critical to improve the semi-variogram calculation and use the kriging variance to effectively quantify estimation uncertainty (Chiles and Delfiner, 2012). After estimating the spatial distribution of log-normal CO₂ concentrations, the inverted log-normal function was applied to obtain maps with the original unit. Finally, besides the mean values map obtained (cell of 50 m • 50 m) from the 100 realizations, the probability map of exceeding the local NBLs was also realized.

4. Results and discussion

4.1. CO₂ emission and geostatistical elaboration

The CO₂ flux values (Table 2S) span over a wide range, between 1.07 g • m⁻² • d⁻¹ and 275 g • m⁻² • d⁻¹.

Statistical approaches were applied to discriminate different CO₂ flux populations. Once the pre-selection criteria were chosen (see Section 3), the dataset appeared non-normally distributed. Multiple populations were highlighted by using the cumulative probability plot shown in Fig. 3a. By applying the partitioning method of Sinclair (1974), three sample populations, namely A1 (n. 56), A2 (n. 338) and B (n. 50), were identified (Fig. 3 and Table 3S). The thresholds, identified based on graphical evidence, were set at 2.41 g • m⁻² • d⁻¹ and 22.04 g • m⁻² • d⁻¹, respectively for A1-A2 and A2-B limits (Fig. 3). The goodness of the choice of thresholds lies in the parametric distribution (log-normal) found for the three identified populations (Fig. 3b).

Pop. A1 shows the lowest CO₂ fluxes with a mean value of 1.85 g • m⁻² • d⁻¹ (min of 1.07 g • m⁻² • d⁻¹, max of 2.41 g • m⁻² • d⁻¹ and median of 1.84 g • m⁻² • d⁻¹), Pop A2 intermediate fluxes has a mean value of 8.37 g • m⁻² • d⁻¹ (min of 2.58 g • m⁻² • d⁻¹, max of 22.04 g • m⁻² • d⁻¹ and median of 7.37 g • m⁻² • d⁻¹) whereas, Pop. B shows the highest CO₂ fluxes with a mean value of 63.65 g • m⁻² • d⁻¹ (min of 23.2 g • m⁻² • d⁻¹, max of 194 g • m⁻² • d⁻¹ and median of 49 g • m⁻² • d⁻¹).

To evaluate the spatial distribution of the CO₂ emissions, an interpolated map was reconstructed (Fig. 4, mean flux values), highlighting the maximum CO₂ flux along a W-E oriented area extending from the mouth of the Crati river to about 5 km towards the inland sectors. On the other hand, as expected, minimum values occur in proximity of the boundaries of the study area, where Pliocene clays are closer to the surface and act as an impermeable layer reducing the overall flux. Anomalous values (higher than those due to soil respiration) are also found along NE-SW oriented lines in the southern sector of the study area, in proximity to the hypothesized main fault systems.

A comparison between flux (Fig. 4) and land use (Fig. 1c) maps does not reveal a specific correlation. The SCP shows an almost homogeneous agricultural activity focused mainly on citrus fruits and rice.

Pop. A2 is the most representative (338) and could represent the

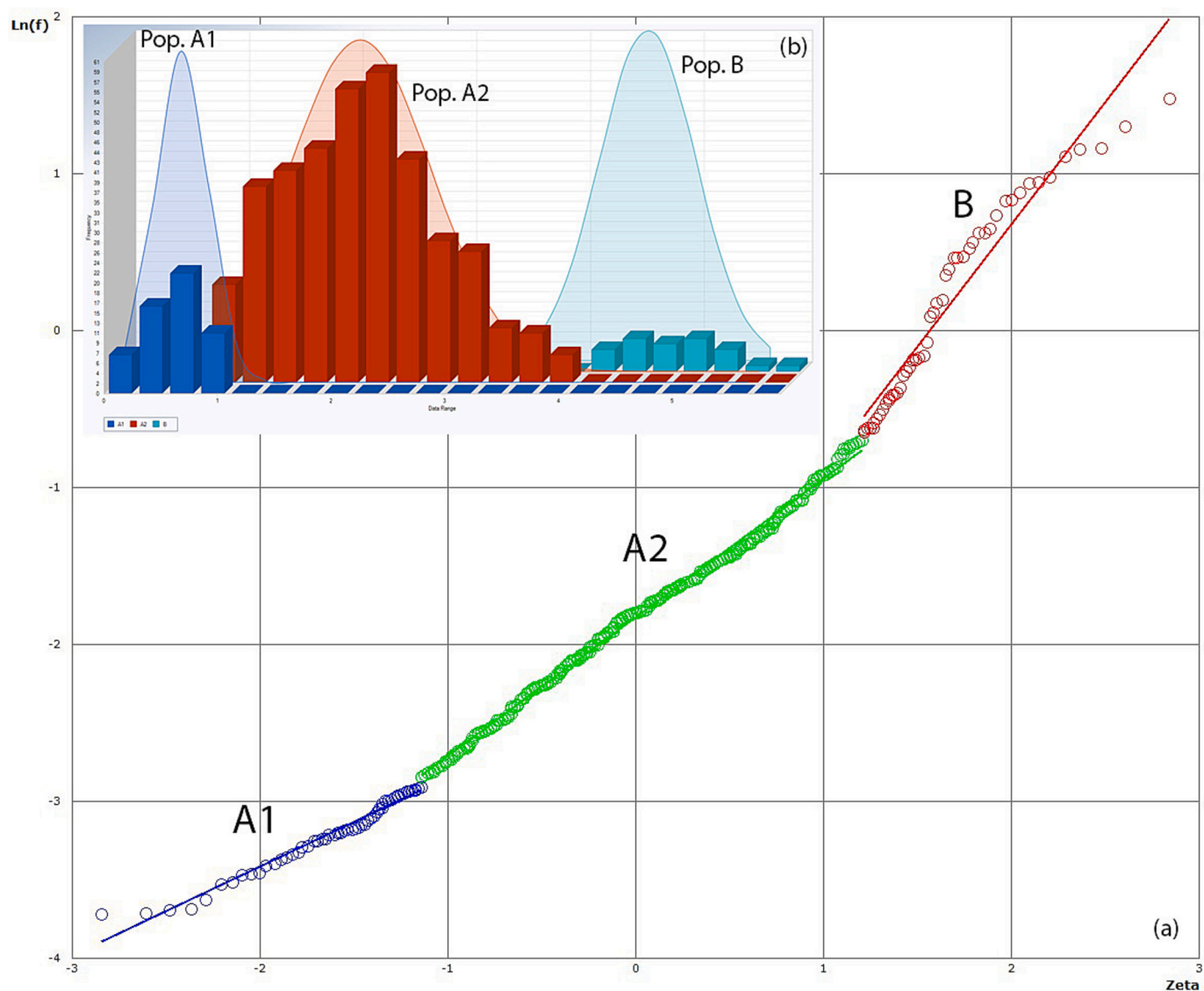


Fig. 3. (a) Graph obtained with the Sinclair method, where three datasets are visible, i.e., “Pop. A1”, Pop. A2” and “Pop. B”. (b) Log-transformed histogram of Pop. A1, A2 and B.

typical range of local vegetation value. It is distributed over all the extent of the study area with minimum values in the proximity of the inland portions, especially where clay units approximate the surface and where, in the northern sector, due to rice cultivation, saturated soil could limit the overall CO_2 flux. In contrast, maximum values are found along the southern sector of the plain along NE-SW oriented alignments coinciding with the strike and intersection of the main faults.

Pop. A1 is less numerous (56) and can represent a sub-group of the local background. The differences between Pop A1 and Pop A2 can be attributed to different local conditions such as vegetation, land use, and/or respiration processes. Low values could be related to sparsely vegetated areas or localized reduced soil permeability with the possible presence of compact clay as reported by Cianflone et al. (2018).

Pop. B yields the highest flux (mean of $63.65 \text{ g} \cdot \text{m}^{-2} \cdot \text{d}^{-1}$). As highlighted in Fig. 4, the high fluxes follow an E-W direction extending from the mouth of the Crati river up to about 5 km towards the inland sectors. The high flux values of Pop. B only partially overlap the main structures characterizing the mouth of the Crati River (Crati and Timparelle faults, and the Sibari Fault Zone) thus preventing a direct correlation. Evidence of the role of faults is found in deep wells (2 onshore exploration wells, *Ogliastrello 001 dir.* and *Thurio 001* wells - VIDEPI

“Visibility of Petroleum Exploration data in Italy”) where gas occurrences are reported along the stratigraphic column between 700 and 800 m b.g.l. These gases could find preferential pathways in the fault systems.

To explain the anomalous values, our hypothesis considers different sedimentary successions characterizing the area, particularly the presence of significant peat levels (up to 3 m thick) found in some wells (Cherubini et al., 2000, ViDEPI, Cianflone et al., 2018). In fact, there is a spatial correlation between Pop. B and the location of wells characterized by peat levels (Fig. 4), which organic matter, during the diagenetic process, can produce CO_2 , e.g. by the reaction:



The presence of organic matter in the area immediately north of the “Parco del Cavallo” archaeological site (ancient Sybaris) can be attributed to ancient lagoonal-depressed areas, that accommodated large amounts of sediment.

The only exception, regarding high flux, is the portions in the proximity of *crati_1*, *crati_2* and *log_A* wells (Fig. 4) located in the *Sibari Lakes* area. In this portion, low fluxes are probably due to a decrease in the gas transport pattern referable to water saturation in the soil pores

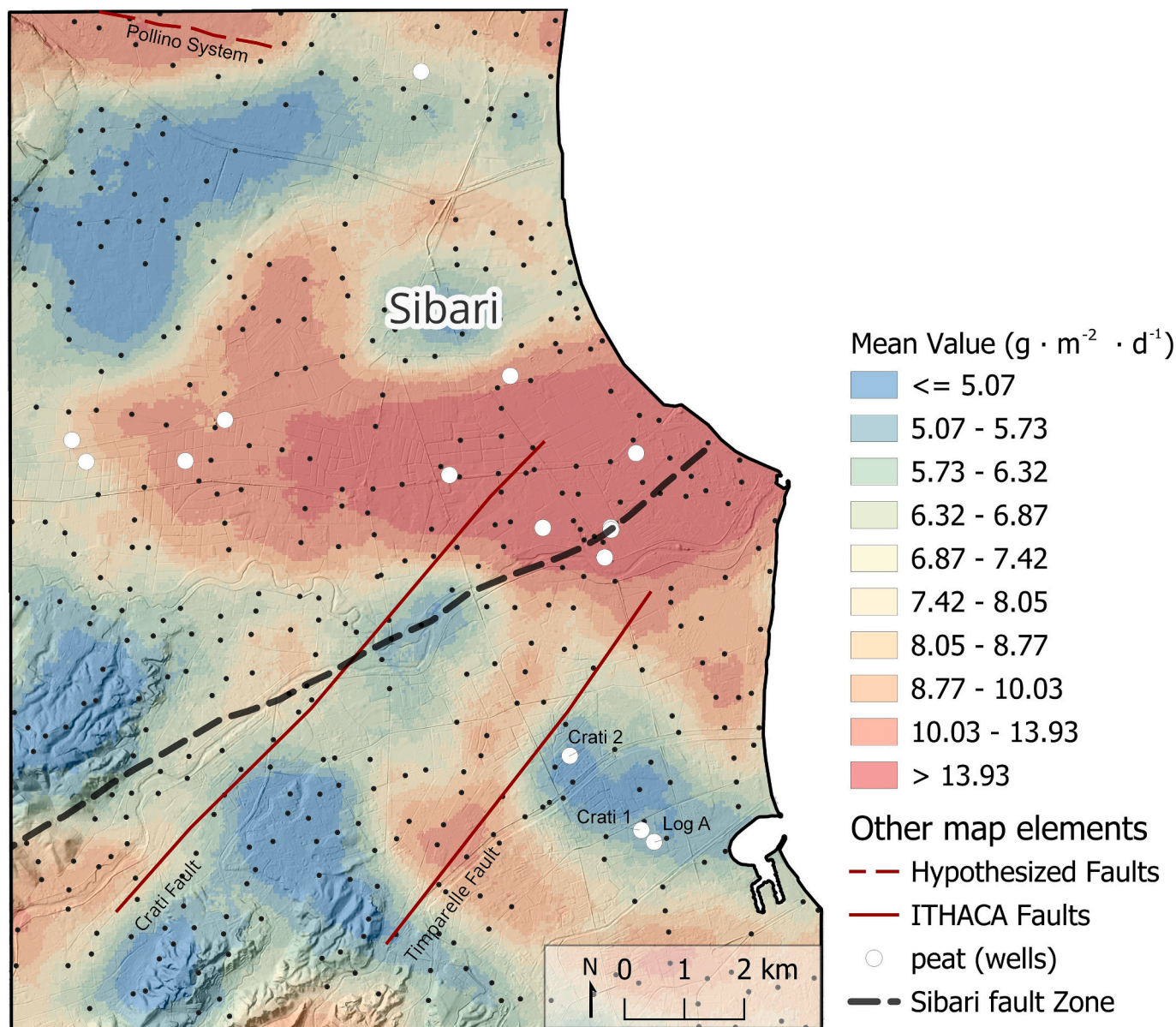


Fig. 4. CO₂ mean flux distribution computed from sGs estimations (100 realizations; cell of 50 m • 50 m). In the map are reported measurement points, main fault systems and wells (white circles) that showed, during digging processes, the presence of peat levels.

(Pérez-Zárate et al., 2024).

4.2. Natural background levels and total CO₂ emissions

The natural background level of CO₂ flux was calculated for population A2 (mean value of 8.37 g • m⁻² • d⁻¹) assumed to be representative of the natural/biological background of the study area. The 95th percentile value of 17.76 g • m⁻² • d⁻¹ was identified (Table 3S). These values are comparable with those reported in literature for typical soil respiration (Cardellini et al., 2003; Shaufler et al., 2010; Correia et al., 2012; Oertel et al., 2016). Harvey et al. (2014) provide comparable average values of biological fluxes for geothermal areas (15.9 g • m⁻² • d⁻¹) and from the Soil Respiration Database (SRDB) values of 8.2 g • m⁻² • d⁻¹ for Mediterranean climate areas and 13 g • m⁻² • d⁻¹ in tropical areas. The natural background values are also consistent with those reported by Raich and Schlesinger (1992) for Mediterranean brush and croplands (7.2 and 5.5 g • m⁻² • d⁻¹, respectively). This suggests that population A2 represents the background level, and confirms that population B is unrelated to soil respiration.

The contribution of CO₂ release from each population discretized by the GSA (Fig. 3) was: i) 45 t • d⁻¹ (43–48 t • d⁻¹) from A1, ii) 1239 t • d⁻¹ (1151–1352 t • d⁻¹) from A2, and 1387 t • d⁻¹ (1199–1672 t • d⁻¹) from B. Thus, the total computed CO₂ emission from the soil of the study area (197 km²) was 2671 t • d⁻¹ (with the 95 % confidence interval of 2393–3071 t • d⁻¹).

Besides the map of mean values obtained through sequential Gaussian simulations, a probability map exceeding the 17.76 g • m⁻² • d⁻¹ threshold of population A2, was also produced (Fig. 5). Even if it is not possible to separate different CO₂ sources, the map clearly shows the presence of localized linear patterns of CO₂ fluxes likely controlled by the concurrence of thick peat levels (also metric) and tectonic structures suggesting that the rise of CO₂ is driven by normal faults that play the role of a preferential circulation pathway for fluids. The geochemical study by Vespasiano et al. (2019) shows how the tectonic structure in this area could allow the circulation of brackish-chloride water from the deep portions of the plain. This additional evidence confirms the presence and role of the fault system previously hypothesized by several authors (Guerricchio et al., 1976; Polemio and Luise, 2007; Vespasiano

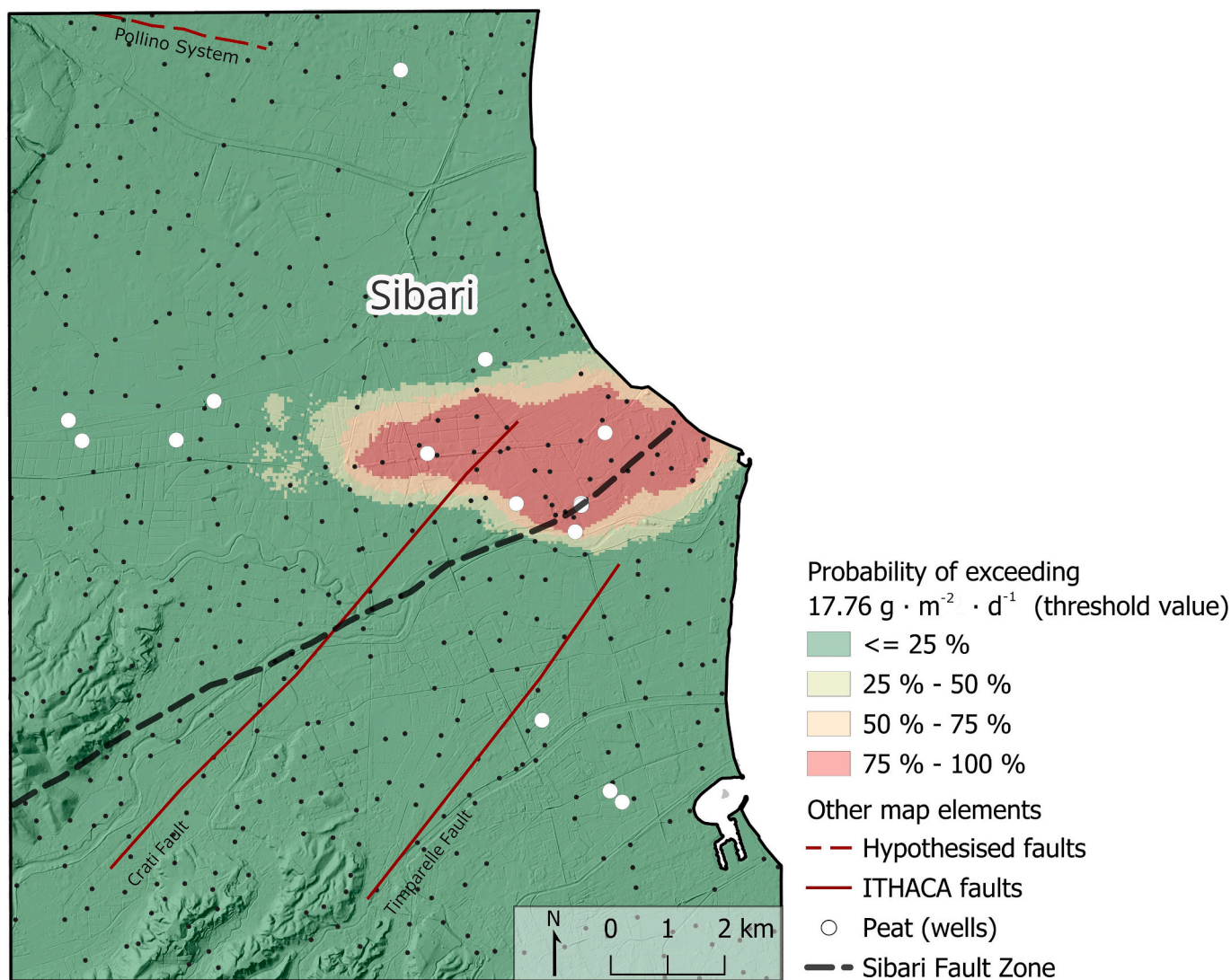


Fig. 5. Probability map of CO₂ flux created through the sequential Gaussian simulations and simple kriging as interpolation method. The map shows the probability that the measured value is greater than a threshold value, specifically $17.76 \text{ g} \cdot \text{m}^{-2} \cdot \text{d}^{-1}$.

et al., 2015a; Vespasiano et al., 2019).

4.3. Comparison between volcanic and non-volcanic CO₂ emissions

GHGs naturally emitted by different soils are widely studied. In particular, the main topic in historical studies is related to volcanic and geothermal emissions, though in recent times natural emissions from different biomes have also been investigated (Cardellini et al., 2003; Camarda et al., 2016; Liu et al., 2023). This allows a comparison between different geological frameworks. In this work, a comparison between volcanic and non-volcanic areas of the Mediterranean area was made to evaluate different specific fluxes that depend on tectonic structures, peat levels, hydrogeological patterns, land use, type of crops, fertilization, and other factors. In terms of overall fluxes, the specific emission recognized along the study area is relatively low ($14.36 \text{ g} \cdot \text{m}^{-2} \cdot \text{d}^{-1}$) if compared with non-volcanic areas that nevertheless are representative of values not negligible for the overall carbon balance like specific areas of Sicily (Madonie System: $60 \text{ g} \cdot \text{m}^{-2} \cdot \text{d}^{-1}$; Peloritani System: $42 \text{ g} \cdot \text{m}^{-2} \cdot \text{d}^{-1}$; Nebrodi System: $121 \text{ g} \cdot \text{m}^{-2} \cdot \text{d}^{-1}$; Hyblean System: $78 \text{ g} \cdot \text{m}^{-2} \cdot \text{d}^{-1}$; Camarda et al., 2016). If only Pop. B is considered, the specific mean flux value increases to $63.65 \text{ g} \cdot \text{m}^{-2} \cdot \text{d}^{-1}$. This value is, as expected, lower than the fluxes emitted from the main volcanic regions Bagni di San Filippo, Mount Amiata (Bollere: 880

$\text{g} \cdot \text{m}^{-2} \cdot \text{d}^{-1}$; Chiodini et al., 2020), Pozzuoli Solfatara ($1300 \text{ g} \cdot \text{m}^{-2} \cdot \text{d}^{-1}$; Cardellini et al., 2003) or Vulcano cone ($1720 \text{ g} \cdot \text{m}^{-2} \cdot \text{d}^{-1}$; Inguaggiato et al., 2022), but on the same order of magnitude of fluxes measured in other volcanic or non-volcanic geothermal areas (e.g., Nisyros Caldera with $39.7 \text{ g} \cdot \text{m}^{-2} \cdot \text{d}^{-1}$; Cardellini et al., 2003; Vesuvio cone with $20 \text{ g} \cdot \text{m}^{-2} \cdot \text{d}^{-1}$; Cardellini et al., 2003) (Fig. 6). This investigation on the SCP makes these CO₂ anomalous fluxes worthy of attention as they are linked to a significant increase of organic matter, a common condition in areas with a similar sedimentary context.

In addition, the normalized total CO₂ output ($\text{t} \cdot \text{d}^{-1} \cdot \text{km}^{-2}$) were compared with areas for which a normalized flux value was provided. Values normalized for the study area (197 km^2) make it possible to compare areas with different extents. As reported by several authors, this value can be calculated by dividing the total CO₂ output for the surface of every site (Werner and Cardellini, 2006; Taussi et al., 2023; Tardani et al., 2024). Considering the value of $2671 \text{ t} \cdot \text{d}^{-1}$ as the total CO₂ output of the Sibari Coastal Plain (given by the sum of the geogenic CO₂ flux and the soil background respiration), the normalized total CO₂ output was then estimated ($13.6 \text{ t} \cdot \text{d}^{-1} \cdot \text{km}^{-2}$) and compared (Table 1) with literature values for different geographic and geological contexts (Cardellini et al., 2003; Werner et al., 2004; Pecoraino et al., 2005; Fridriksson et al., 2006; Chiodini et al., 2007; Dereinda, 2008; Werner et al., 2008; Jácome-Paz et al., 2019; Chiodini et al., 2020; Sbrana et al.,

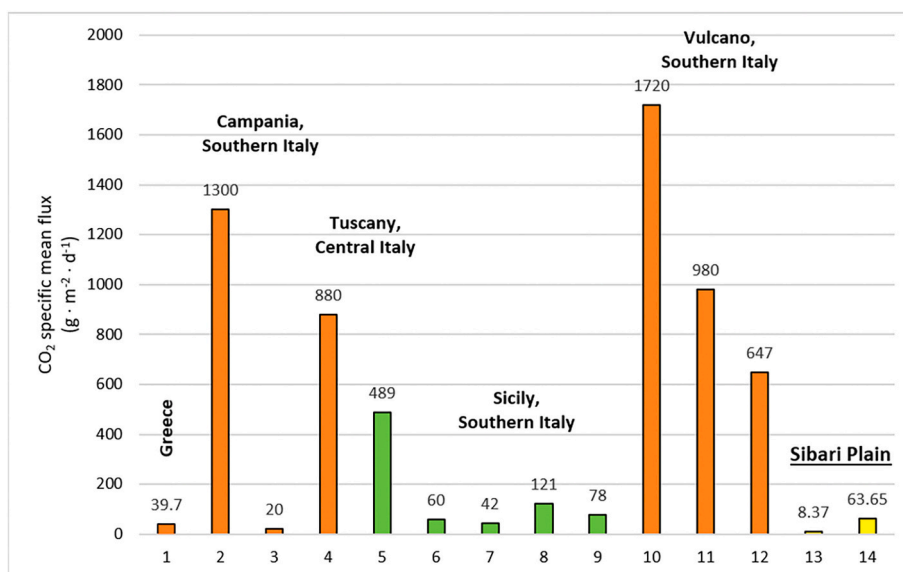


Fig. 6. Comparison between volcanic CO₂ emissions (in orange) and non-volcanic CO₂ emissions (in green), from different areas (on the top of the columns are the average specific fluxes). The values are expressed in $\text{g} \cdot \text{m}^{-2} \cdot \text{d}^{-1}$. In detail: 1 - Nisyros Caldera from Cardellini et al. (2003); 2 - Pozzuoli solfatara from Cardellini et al. (2003); 3 - Vesuvio cone from Cardellini et al. (2003); 4 - Bagni di San Filippo (Bollere) from Chiodini et al. (2020); 5 - Poggio dell'Olivo from Cardellini et al. (2003); 6 - Madonie System (M1) from Camarda et al. (2016); 7 - Peloritani System (NP1) from Camarda et al. (2016); 8 - Nebrodi System (N2) from Camarda et al. (2016); 9 - Hyblean System (H5) from Camarda et al. (2016); 10 - Vulcano cone from Inguaggiato et al. (2022); 11 - Palizzi area (Vulcano) from Inguaggiato et al. (2022); 12 - Levante Bay area (Vulcano) from Inguaggiato et al. (2022); 13 - Sibari Plain (Pop. A2) from this work; 14 - Sibari Plain (Pop. B) from this work (in yellow).

2020; Taussi et al., 2023). As shown by Table 1, the value characterizing the Sibari plain is low, but comparable with data obtained in other critical geological contexts (also volcanic) e.g., Lagoni - Sasso Pisano, $32.75 \text{ t} \cdot \text{d}^{-1} \cdot \text{km}^{-2}$ (Tuscany - Italy); Vesuvio cone and Ischia, 21.47 and $28.17 \text{ t} \cdot \text{d}^{-1} \cdot \text{km}^{-2}$, respectively (Campania - Italy); Agua Caliente, $16 \text{ t} \cdot \text{d}^{-1} \cdot \text{km}^{-2}$ (Mexico) and Karapiti, Wairakei $17.71 \text{ t} \cdot \text{d}^{-1} \cdot \text{km}^{-2}$ (New Zealand).

4.4. CH₄ emissions

Out of 459 total measurements, there are only three recorded values of CH₄ above the instrumental detection limit of $0.032 \text{ g} \cdot \text{m}^{-2} \cdot \text{d}^{-1}$. These do not appear to be directly related to areas of high CO₂ flux. Stratigraphic data indicates that peat strata are common in the Sibari Plain and may be considered candidates for local methane emissions. Stratigraphic heterogeneity is reported in the plain, which may affect biochemical processes involved in methane production and release. In terms of natural consumption, methane can be oxidized by methanotrophic microorganisms using oxygen or alternative terminal electron acceptors. In aerobic conditions methane can be utilized by bacteria belonging to the phyla *Proteobacteria* and *Verrucomicrobia*, while in anaerobic conditions methane oxidation is mediated by anaerobic methanotrophs belonging to both bacteria and archaea domains (Guerrero-Cruz et al., 2021). In aerobiosis, the O₂ (surface conditions) reacts with CH₄ and release both CO₂ and H₂O ($\text{CH}_4 + 2\text{O}_2 \rightarrow \text{CO}_2 + 2\text{H}_2\text{O}$) (Serrano-Silva et al., 2014).

Methanotrophic bacteria proliferating on the interface between reducing and oxidizing conditions can consume up to 80 % of the total CH₄ output (Conrad, 2009). Vespasiano et al. (2019), studying the aquifers of the Sibari Plain, reported a variable interface between reducing and oxidizing conditions, which may favors the development of methanotrophic bacteria involved in the consumption of the released CH₄. Furthermore, Pliocene clay levels could be a permeability threshold to gas ascension. These assumptions can help explain the absence of surface CH₄ on the Sibari Plain.

It is worth noting that all points were located far from settlements, so the possibility of natural gas supply network leaks can be excluded.

Additionally, the fact that most measurements did not yield CH₄ fluxes is deemed significant, as it excludes a characteristic geological framework such as the Sibari Coastal Plain as a possible emitter of methane in Calabria. Considering the uncertainties related - on a global scale - to the total emission output of methane, narrowing down its possible natural emission sources constitutes a step forward towards a better understanding of the global methane budget.

5. Conclusion and potential implications

The Sibari Coastal Plain is one of the most interesting areas in Calabria (Southern Italy) for studying non-volcanic soil emissions due to its geological, stratigraphic, and structural framework. The aim of this work was focused on the measurement of natural gas emissions from soils to assess (i) anomalous fluxes in terms of CO₂ and CH₄ along a selected portion of the Sibari Plain, (ii) the relationship between emitted gases, organic matter, tectonic structures, and (iii) the potential environmental implications. Carbon dioxide flux values, distributed along the SCP, fall in a wide range between $1.07 \text{ g} \cdot \text{m}^{-2} \cdot \text{d}^{-1}$ and $275 \text{ g} \cdot \text{m}^{-2} \cdot \text{d}^{-1}$, with the highest values recognized in proximity to the mouth of the Crati River and the lowest ones along the inner sectors, where Pliocene clays are closer to the surface. On the other hand, CH₄ yields values mainly below the detection limit of $0.032 \text{ g} \cdot \text{m}^{-2} \cdot \text{d}^{-1}$. The absence of CH₄ emission can be related to taphonomic processes of organic-rich sediments and peat or possible consumption by methanotrophic organisms. Moreover, clay levels separating the shallow aquifer from the deeper one could be a permeability threshold to gas uprising.

Statistical and geostatistical approaches allowed the discrimination of three main CO₂ flux populations: Pop. A1 representative of the lowest CO₂ fluxes (mean value of $1.85 \text{ g} \cdot \text{m}^{-2} \cdot \text{d}^{-1}$), Pop. A2 with intermediate flux (mean value of $8.37 \text{ g} \cdot \text{m}^{-2} \cdot \text{d}^{-1}$), and Pop. B showing the highest CO₂ flux (mean value of $63.65 \text{ g} \cdot \text{m}^{-2} \cdot \text{d}^{-1}$).

Pop. A2 (NBL $17.76 \text{ g} \cdot \text{m}^{-2} \cdot \text{d}^{-1}$) can be attributed to normal soil respiration. Pop. B, on the other hand, falls entirely along the inner sector of the mouth of the Crati River, showing a good correlation with deep peat levels recognized in previous works. The concomitant presence of faults, even overlapped, and thick peat levels (even metric)

Table 1

Comparison between “Normalized CO₂ total output” from different places worldwide.

Site	Locality	Norm. TOT Output ($t \cdot d^{-1} \cdot km^{-2}$)	Reference
Sibari Plain	Calabria, Italy	13.6	<i>This Work</i>
Mt. Amiata		59.0	Sbrana et al., 2020
Sasso Pisano		211.3	Taussi et al., 2023
Sasso		74.6	Taussi et al., 2023
Monterotondo		268.8	Taussi et al., 2023
Lagoni - Sasso Pisano		32.8	Taussi et al., 2023
Micciano NW area	Tuscany, Italy	344.8	Taussi et al., 2023
Micciano SE area		144.4	Taussi et al., 2023
Libbiano		699.2	Taussi et al., 2023
Palazzo al Piano		118.4	Taussi et al., 2023
Montemiccioli		1320.6	Taussi et al., 2023
Poggio dell'Olivo		308.7	Cardellini et al., 2003
Bagni San Filippo		508.8	Chioldini et al., 2020
Latera	Latium, Italy	160.3	Chioldini et al., 2007
Solfatara of Pozzuoli		1103.2	Cardellini et al., 2003
Vesuvio cone	Campania, Italy	21.5	Cardellini et al., 2003
Ischia		28.2	Pecoraino et al., 2005
Nisyros caldera	Greece	42.0	Cardellini et al., 2003
Krafla		41.8	Dereinda, 2008
Reykjanes	Iceland	60.4	Fridriksson et al., 2006
La Escalera	Mexico	63.0	Jácome-Paz et al., 2019
Agua Caliente		16.0	Jácome-Paz et al., 2019
Yellowstone caldera	USA	2562	Werner et al., 2008
Horseshoe Lake		962.3	Cardellini et al., 2003
Karapiti, Wairakei	New Zealand	17.7	Werner et al., 2004

favors the development of flows that deviate considerably from local background values, allowing to confirm the presence of tectonic structures initially hypothesized by several authors along the inner sectors of the mouth of the Crati River.

Considering the extent of the Sibari Plain (197 km²), a total CO₂ flow of about 2671 t • d⁻¹ was calculated, which, if compared to the total flow expected for the simple soil respiration (i.e., from populations A1 and A2: 1284 t • d⁻¹), represents a non-negligible value in the total balance. Furthermore, a comparison between specific fluxes and normalized output measured by previous authors in volcanic and non-volcanic areas was performed. In terms of overall fluxes, specific flux is relatively low (14.36 g • m⁻² • d⁻¹) compared to non-volcanic and volcanic regions. Nevertheless, if only Pop. B is considered, the specific flux increases up to 63.65 g • m⁻² • d⁻¹, a value comparable to (or higher than) fluxes measured in other volcanic, non-volcanic or geothermal areas. Finally, the estimated Total Normalized CO₂ output (13.6 t • d⁻¹ • km⁻²) is similar to the data obtained in other critical geological contexts, including those of volcanic origin. The results imply that the contribution of coastal plains in terms of atmospheric CO₂ emissions needs to be considered. Carbon dioxide soil emissions in the investigated area appear to be mainly related to (i) accumulations of organic matter (as reported in similar geological contexts), and (ii) a complex tectonic framework. Both these contributions can lead to anomalous CO₂ emissions in coastal plains.

This work represents one of the first attempts aimed at the

understanding of the role played by coastal plains in terms of GHGs emissions. The proposed method may be used in similar contexts to implement the knowledge of these kinds of environments and quantify the soil CO₂ contribution in terms of total emission outputs. Finally, this study may also be considered the starting point for future research accounting for extra information on both CO₂ and CH₄, such as carbon isotope values and fractionation processes, since the sources of either compound have characteristic isotopic fingerprints which can be of paramount importance in the effort of evaluating their origin.

Supplementary data to this article can be found online at <https://doi.org/10.1016/j.scitotenv.2025.178611>.

CRedit authorship contribution statement

C. Apollaro: Writing – review & editing, Writing – original draft, Validation, Supervision, Software, Resources, Project administration, Methodology, Investigation, Funding acquisition, Formal analysis, Data curation, Conceptualization. **G. Vespasiano:** Writing – review & editing, Writing – original draft, Visualization, Validation, Supervision, Software, Resources, Project administration, Methodology, Investigation, Formal analysis, Data curation, Conceptualization. **I. Fuoco:** Writing – review & editing, Writing – original draft, Visualization, Validation, Supervision, Software, Resources, Project administration, Methodology, Formal analysis, Data curation, Conceptualization. **M. Taussi:** Writing – review & editing, Writing – original draft, Validation, Software, Methodology, Formal analysis, Data curation, Conceptualization. **R. De Rosa:** Writing – review & editing, Writing – original draft, Validation, Supervision, Funding acquisition. **M.F. La Russa:** Writing – review & editing, Writing – original draft, Validation, Supervision, Funding acquisition. **A. Guido:** Writing – review & editing, Writing – original draft, Supervision, Methodology, Formal analysis, Data curation, Conceptualization. **D. Di Curzio:** Writing – review & editing, Writing – original draft, Validation, Supervision. **A. Renzulli:** Writing – review & editing, Writing – original draft, Validation, Supervision. **L. Russo:** Writing – review & editing, Writing – original draft, Software, Methodology, Investigation, Formal analysis, Data curation. **F. Ciniglia:** Writing – review & editing, Writing – original draft, Software, Methodology, Investigation, Formal analysis, Data curation. **F. D’Amico:** Writing – review & editing, Writing – original draft, Software, Methodology, Investigation, Formal analysis, Data curation. **M. Cipriani:** Writing – review & editing, Writing – original draft, Validation, Software, Methodology, Formal analysis, Data curation. **G. Maruca:** Writing – review & editing, Writing – original draft, Validation, Software, Methodology, Formal analysis, Data curation. **G. Virgili:** Writing – review & editing, Writing – original draft, Software, Methodology, Formal analysis, Data curation. **A. Bloise:** Writing – review & editing, Writing – original draft, Supervision, Methodology, Funding acquisition, Formal analysis, Data curation, Conceptualization.

Declaration of competing interest

The authors declare that they have no known competing financial interests or personal relationships that could have appeared to influence the work reported in this paper.

Acknowledgements

This work was funded by the Next Generation EU - Italian NRRP, Mission 4, Component 2, Investment 1.5, call for the creation and strengthening of ‘Innovation Ecosystems’, building ‘Territorial R&D Leaders’ (Directorial Decree n. 2021/3277) - project Tech4You - Technologies for climate change adaptation and quality of life improvement, n. ECS0000009 and PRIN 2022 PNRR-Thermal model of Aeolian Islands for new perspectives of sustainable exploitation of geothermal resources”, CUP H53D23011420001. This work reflects only the authors’ views and opinions, neither the Ministry for University and Research nor

the European Commission can be considered responsible for them.

Dr. Salvatore Inguaggiato (INGV Palermo) and two anonymous reviewers are acknowledged for their constructive comments that helped improve a previous version of the manuscript. We are also grateful to the associate editor for handling the manuscript. ArcGIS was used under a license provided to the University of Urbino.

Data availability

Data will be made available on request.

References

- Apollaro, C., Marini, L., De Rosa, R., 2007a. Use of reaction path modeling to predict the chemistry of stream water and groundwater: a case study from the Fiume Grande valley (Calabria, Italy). *Environ. Geol.* 51, 1133–1145.
- Apollaro, C., Marini, L., De Rosa, R., Settembrino, P., Scarciglia, F., Vecchio, G., 2007b. Geochemical features of rocks, stream sediments, and soils of the Fiume Grande Valley (Calabria, Italy). *Environ. Geol.* 52, 719–729.
- Apollaro, C., Buccianti, A., Vespasiano, G., Vardè, M., Fuoco, I., Barca, D., Bloise, A., Miriello, D., Cofone, F., Servidio, A., De Rosa, R., 2019. Comparative geochemical study between the tap waters and the bottled mineral waters in Calabria (southern Italy) by compositional data analysis (CoDA) developments. *Appl. Geochem.* 107, 19–33.
- Apollaro, C., Caracausi, A., Paternoster, M., Randazzo, P., Aiuppa, A., De Rosa, R., Fuoco, I., Mongelli, G., Muto, F., Vanni, E., Vespasiano, G., 2020. Fluid geochemistry in a low-enthalpy geothermal field along a sector of southern Apennines chain (Italy). *J. Geochem. Explor.* 219, 106618.
- Apollaro, C., Fuoco, I., Gennaro, E., Giuliani, L., Iezzi, G., Marini, L., Radica, F., Di Luccio, F., Ventura, G., Vespasiano, G., 2023. Advanced argillic alteration at cave di Caolino, Lipari, Aeolian Islands (Italy): implications for the mitigation of volcanic risks and the exploitation of geothermal resources. *Sci. Total Environ.* 889, 164333.
- Aselmann, I., Crutzen, P.J., 1990. A global inventory of wetland distribution and seasonality, net primary productivity and estimated methane emissions. In: Bouwman, A.F. (Ed.), *Soils and the Greenhouse Effect*. John Wiley & Sons Ltd, Chichester, pp. 441–449.
- Barnes, I., Irwin, W.P., White, D., 1978. Global distribution of carbon-dioxide discharges and major zones of seismicity. In: WRL 78. US geological survey, Water Resource Division. <https://doi.org/10.3133/wri7839>.
- Battagliani, R., Raco, B., Scozzari, A., 2013. Effective monitoring of landfills: flux measurements and thermography enhance efficiency and reduce environmental impact. *J. Geophys. Eng.* 10 (6), 064002. <https://doi.org/10.1088/1742-2132/10/6/064002>.
- Baubron, J.C., Rigo, A., Toutain, J.P., 2002. Soil gas profiles as a tool to characterize active tectonic areas: the Jaut pass example (Pyrenees, France). *Earth Planet. Sci. Lett.* 196 (1–2), 69–81. [https://doi.org/10.1016/S0012-821X\(01\)00596-9](https://doi.org/10.1016/S0012-821X(01)00596-9).
- Blunden, J., Boyer, T., Bartow-Gillies, E., 2023. State of the climate in 2022. *B. Am. Meteorol. Soc.* 104 (9), 1–501. <https://doi.org/10.1175/2023BAMSStateoftheClimate.1>.
- Byrom, R.E., Shine, K.P., 2022. Methane's solar radiative forcing. *Geophys. Res. Lett.* 49 (15), e2022GL098270. <https://doi.org/10.1029/2022GL098270>.
- Camarda, M., De Gregorio, S., Roberto, M., Di Martino, R., Favara, R., 2016. Temporal and spatial correlation between soil CO₂ flux and crustal stress. *J. Geophys. Res.* 121, 7071–7085. <https://doi.org/10.1002/2016JB013297>.
- Cannata, C.B., Cianflone, G., Vespasiano, G., De Rosa, R., 2016. Preliminary analysis of sediments pollution of the coastal sector between Crotona and Strongoli (Calabria - southern Italy). *Rend. Online. Soc. Geol. Ital.* 38, 17–20. <https://doi.org/10.3301/ROL.2016.06>.
- Caracausi, A., Michele, P., Pasquale, M.N., 2015. Mantle CO₂ degassing at Mt. Vulture volcano (Italy): relationship between CO₂ outgassing of volcanoes and the time of their last eruption. *Earth Planet. Sci. Lett.* 411, 268–280. <https://doi.org/10.1016/j.epsl.2014.11.049>.
- Carapezza, M.L., Ranaldi, M., Gattuso, A., Pagliuca, N.M., Tarchini, L., 2015. The sealing capacity of the cap rock above the Torre Alfina geothermal reservoir (Central Italy) revealed by soil CO₂ flux investigations. *J. Volcanol. Geotherm. Res.* 291, 25–34. <https://doi.org/10.1016/j.jvolgeores.2014.12.011>.
- Cardellini, C., Chiodini, G., Frondini, F., 2003. Application of stochastic simulation to CO₂ flux from soil: mapping and quantification of gas release. *J. Geophys. Res. Solid Earth* 108 (B9). <https://doi.org/10.1029/2002JB002165>.
- Cardellini, C., Chiodini, G., Frondini, F., Avino, R., Bagnato, E., Caliro, S., Lelli, M., Rosiello, A., 2017. Monitoring diffuse volcanic degassing during volcanic unrest: the case of Campi Flegrei (Italy). *Sci. Rep.* 7 (1), 6757. <https://doi.org/10.1038/s41598-017-06941-2>.
- Cherubini, C., Cotecchia, V., Pagliarulo, R., 2000. Subsidence in the Sibari plain (Italy). *Land Subsidence. Proceedings of the Sixth International Symposium on Land Subsidence* 1, 3–15.
- Chiles, J.P., Delfiner, P., 2012. *Geostatistics: Modeling Spatial Uncertainty*. John Wiley & Sons.
- Chiodini, G., Cioni, R., Guidi, M., Raco, B., Marini, L., 1998. Soil CO₂ flux measurements in volcanic and geothermal areas. *Appl. Geochem.* 13, 543–552. [https://doi.org/10.1016/S0883-2927\(97\)00076-0](https://doi.org/10.1016/S0883-2927(97)00076-0).
- Chiodini, G., Baldini, A., Barberi, F., Carapezza, M.L., Cardellini, C., Frondini, F., Granieri, D., Ranaldi, M., 2007. Carbon dioxide degassing at latera caldera (Italy): evidence of geothermal reservoir and evaluation of its potential energy. *J. Geophys. Res. Solid Earth* 112. <https://doi.org/10.1029/2006JB004896>.
- Chiodini, G., Cardellini, C., Caliro, S., Avino, R., Donnini, M., Granieri, D., Morgantini, N., Sorrenti, D., Frondini, F., 2020. The hydrothermal system of Bagni san Filippo (Italy): fluids circulation and CO₂ degassing. *IJG* 139, 383–397. <https://doi.org/10.3301/IJG.2020.12>.
- Cianflone, G., Dominici, R., Apollaro, C., De Rosa, R., Polemio, M., Romanazzo, A., Vespasiano, G., 2013. Preliminary study of holocenic geological evolution of the lower Crati Valley. Quantitative and qualitative assessment of groundwater resources: standard methods, new developments and open problem. In: *FIST GEOTITALIA 2013 – IX Forum di Scienze della Terra–Pisa*, pp. 260–261.
- Cianflone, G., Tolomei, C., Brunori, C., Dominici, R., 2015. InSAR time series analysis of natural and anthropogenic coastal plain subsidence: the case of Sibari (southern Italy). *Remote Sens.* 12, 16004–16023. <https://doi.org/10.3390/rs1215812>.
- Cianflone, G., Cavuoto, G., Punzo, M., Dominici, R., Sonnino, M., Di Fiore, V., Pelosi, N., Tarallo, D., Lirer, F., Marsella, E., Critelli, S., De Rosa, R., 2018. Late quaternary stratigraphic setting of the Sibari plain (southern Italy): hydrogeological implications. *Mar. Pet. Geol.* 97, 422–436. <https://doi.org/10.1016/j.marpetgeo.2018.07.027>.
- Cianflone, G., Vespasiano, G., De Rosa, R., Dominici, R., Apollaro, C., Vaselli, O., Pizzino, L., Tolomei, C., Capecchiacci, F., Polemio, M., 2021. Hydrostratigraphic framework and physicochemical status of groundwater in the Gioia Tauro coastal plain (Calabria—southern Italy). *Water* 13, 3279. <https://doi.org/10.3390/w1323279>.
- Cianflone, G., Vespasiano, G., Tolomei, C., De Rosa, R., Dominici, R., Apollaro, C., Polemio, M., 2022. Different ground subsidence contributions revealed by integrated discussion of Sentinel-1 datasets, well discharge, stratigraphical and geomorphological data: the case of the Gioia Tauro coastal plain (southern Italy). *Sustainability* 14 (5), 2926. <https://doi.org/10.3390/su14052926>.
- Cinti, F.R., Alfonsi, L., D'Alessio, A., Marino, S., Brunori, C.A., 2015. Faulting and ancient earthquakes at Sybaris archaeological site, ionian Calabria, southern Italy. *Seismol. Res. Lett.* 86, 245–254. <https://doi.org/10.1785/02201401071>.
- Cinti, F.R., Alfonsi, L., Cucci, L., Pantosti, D., Pauselli, C., Ercoli, M., Brunori, C.A., Cianflone, G., Dominici, R., 2024. The NE-SW Sibari fault zone: a seismic hazard source in Ionian northern Calabria (Italy). *Tectonophysics* 873, 230214. <https://doi.org/10.1016/j.tecto.2024.230214>.
- Cipriani, M., Dominici, R., Costanzo, A., D'Antonio, M., Guido, A., 2021. A messinian gypsum deposit in the ionian forearc basin (benestare, Calabria, southern Italy): origin and paleoenvironmental indications. *Minerals* 11 (12), 1305. <https://doi.org/10.3390/min11121305>.
- Cipriani, M., Dominici, R., Costanzo, A., Vespasiano, G., Apollaro, C., Miriello, D., Cianflone, G., Perri, F., D'Antonio, M., Maruca, G., Guido, A., 2023. Messinian resedimented gypsum (branching-like facies) from the Catanzaro Basin (Calabria, southern Italy): petrographic and geochemical evidence for paleoenvironmental reconstruction. *Rend. Online Soc. Geol. Ital.* 59, 35–39. <https://doi.org/10.3301/ROL.2023.06>.
- Cipriani, M., Donato, S., Alessandro, F., Campilongo, G., Cianflone, G., Costanzo, A., Guido, A., Lanzafame, G., Magarò, P., Maletta, C., Maruca, G., Dominici, R., 2024. Can crystal imperfections alter the petrophysical properties of halite minerals? *Mar. Pet. Geol.* 168, 107013. <https://doi.org/10.1016/j.marpetgeo.2024.107013>.
- Cirrincione, R., Fazio, E., Fiannacca, P., Ortolano, G., Pezzino, A., Punturo, R., 2015. The Calabria-Peloritani Orogen, a composite terrane in Central Mediterranean; its overall architecture and geodynamic significance for a pre-alpine scenario around the Tethyan basin. *Periodico di Mineralogia* 84, 701–749. <https://doi.org/10.2451/2015PM0446>.
- Comerci, V., Bumetti, A.M., Di Manna, P., Fiorenza, D., Guerrieri, L., Lucarini, M., Serva, L., Vittori, E., 2013. ITHACA project and capable faults in the Po plain (northern Italy). *Ingegneria Sismica* 30 (1–2), 36–50. *Special Issue*.
- Conrad, R., 2009. The global methane cycle: recent advances in understanding the microbial processes involved. *Environ. Microbiol. Rep.* 1, 285–292. <https://doi.org/10.1111/j.1758-2229.2009.00038.x>.
- Corazza, E., Magro, G., Ceccarelli, A., Pieri, S., Rossi, U., 1993. Soil gas survey in the geothermal area of bolsena lake (Vulsini Mts. Central Italy). *Geothermics* 22, 201–214. [https://doi.org/10.1016/0375-6505\(93\)90043-M](https://doi.org/10.1016/0375-6505(93)90043-M).
- Corine Land Cover (CLC), 2019. <https://land.copernicus.eu/en/products/corine-land-cover>.
- Correia, A.C., Minunno, F., Caldeira, M.C., Banza, J., Mateus, J., Carneiro, M., Wingate, L., Shvaleva, A., Ramos, A., Jongen, M., Bugalho, M.N., Nogueira, C., Lecomte, X., Pereira, J.S., 2012. Soil water availability strongly modulates soil CO₂ efflux in different Mediterranean ecosystems: model calibration using the Bayesian approach. *Agric. Ecosyst. Environ.* 161, 88–100. <https://doi.org/10.1016/j.agee.2012.07.025>.
- Cristofanelli, P., Busetto, M., Calzolari, F., Ammoscato, I., Gulli, D., Dinoi, A., Calidonna, C.R., Contini, D., Sferlazzo, D., Di Iorio, T., Piacentino, S., Marinoni, A., Maione, M., Bonasoni, P., 2017. Investigation of reactive gases and methane variability in the coastal boundary layer of the Central Mediterranean basin. *Elem. Sci. Anth* 5, 12. <https://doi.org/10.1525/elementa.216>.
- David, M., 1977. *Geostatistical Ore Reserve Estimation (Developments in Geomathematics 2)*. Elsevier, New York, p. 363.
- Dereinda, F.H., 2008. *CO₂ Emissions from the Krafla Geothermal Area*. United Nations University Geothermal Training Programme, Reports 2008, Iceland.
- Deutsch, C.V., Journel, A.G., 1992. *Geostatistical software library and user's guide*. N. Y. 119 (147), 578.

- Dickinson, D., Bodé, S., Boeckx, P., 2017. System for $\delta^{13}\text{C}\text{-CO}_2$ and xCO_2 analysis of discrete gas samples by cavity ring-down spectroscopy. *Atmos. Meas. Tech.* 10(11), pgs. 4507–4519. doi:<https://doi.org/10.5194/amt-10-4507-2017>.
- Dinh, T.V., Choi, I.Y., Son, Y.S., Kim, J.C.K., 2016. A review on non-dispersive infrared gas sensors: improvement of sensor detection limit and interference correction. *Sens. Actuators B: Chem.* 231, 529–538. <https://doi.org/10.1016/j.snb.2016.03.040>.
- Elio, J., Ortega, M.F., Nisi, B., Mazadiago, L.F., Vaselli, O., Caballero, J., Chacón, E., 2016. A multi-statistical approach for estimating the total output of CO_2 from diffuse soil degassing by the accumulation chamber method. *Int. J. Greenhouse Gas Control* 47, 351–363.
- Etiopie, G., Feyzullayev, A., Milkov, A.V., Waseda, A., Mizobe, K., Sun, C.H., 2009. Evidence of subsurface anaerobic biodegradation of hydrocarbons and potential secondary methanogenesis in terrestrial mud volcanoes. *Mar. Pet. Geol.* 26(9), 1962–1703. doi:<https://doi.org/10.1016/j.marpetgeo.2008.12.002>.
- Frenzel, P., Karofeld, E., 2000. CH_4 emission from a hollow-ridge complex in a raised bog: the role of CH_4 production and oxidation. *Biogeochemistry* 51, pgs. 91–112. doi:<https://doi.org/10.1023/A:1006351118347>.
- Fridriksson, T., Kristjánsson, B.R., Ármannsson, H., Margrétardóttir, E., Ólafsdóttir, S., Chiodini, G., 2006. CO_2 emissions and heat flow through soil, fumaroles, and steam heated mud pools at the Reykjanes geothermal area, SW Iceland. *Appl. Geochem.* 21 (9), 1551–1569. <https://doi.org/10.1016/j.apgeochem.2006.04.006>.
- Fu, C.C., Yang, T.F., Wallia, V., Chen, C.H., 2005. Reconnaissance of soil gas composition over the buried fault and fracture zone in southern Taiwan. *Geochem. J.* 39 (5), 427–439. <https://doi.org/10.2343/geochemj.39.427>.
- Guerra, M., Lombardi, S., 2001. Soil-gas method for tracing neotectonic fault synclay basins: the Pisticci field (southern Italy). *Tectonophysics* 339 (3–4), 511–522. [https://doi.org/10.1016/S0040-1951\(01\)00072-5](https://doi.org/10.1016/S0040-1951(01)00072-5).
- Guerrero-Cruz, S., Vaksmaa, A., Horn, M.A., Niemann, H., Pijuan, M., Ho, A., 2021. Methanotrophs: discoveries, environmental relevance, and a perspective on current and future applications. *Front. Microbiol.* 12. <https://doi.org/10.3389/fmicb.2021.678057>.
- Guerricchio, A., Melidoro, G., Tazioli, G.S., 1976. Lineamenti idrogeologici e subsidenza dei terreni olocenici della piana di Sibari. *Rivista e sviluppo n. 9* (Cassa di risparmio di Calabria e Lucania Cosenza 77–80).
- Harriss, R.C., Gorham, E., Sebacher, D.L., Bartlett, K.B., Flebbe, P.A., 1985. Methane flux from northern peatlands. *Nature* 315, pgs. 652–654. doi:<https://doi.org/10.1038/315652a0>.
- Harvey, M.C., Britten, K., Schwendenmann, L., 2014. A Review of Approaches to Distinguish between Biological and Geothermal Soil Diffuse CO_2 Flux. In: *New Zealand Geothermal Workshop 2014 Proceedings*.
- He, Y., Bond-Lamberty, B., Myers-Pigg, A.N., Newcomer, M.E., Ladau, J., Holmquist, J. R., Falco, N., 2024. Effects of spatial variability in vegetation phenology, climate, landcover, biodiversity, topography, and soil property on soil respiration across a coastal ecosystem. *Heliyon* 10 (9). <https://doi.org/10.1016/j.heliyon.2024.e30470>.
- Inguaggiato, S., Vita, F., Diliberato, I.S., Inguaggiato, C., Mazot, A., Cangemi, M., Corrao, M., 2022. The volcanic activity changes occurred in the 2021–2022 at Vulcano island (Italy), inferred by the abrupt variations of soil CO_2 output. *Sci. Rep.* 12 (1), 21166. <https://doi.org/10.1038/s41598-022-25435-4>.
- Irwin, W.P., Barnes, I., 1980. Tectonic relations of carbon dioxide discharges and earthquakes. *J. Geophys. Res.* 85, 3115–3121. <https://doi.org/10.1029/JB085iB06p03115>.
- Italiano, F., Pietro, B., Manuela, D., Riccardo, P., Francesca, S., 2009. Helium and carbon isotopes in the dissolved gases of Friuli region (NE Italy): geochemical evidence of CO_2 production and degassing over a seismically active area. *Chem. Geol.* 76–85. <https://doi.org/10.1016/j.chemgeo.2009.05.022>.
- Jácome-Paz, M.P., Pérez-Zárate, D., Prol-Ledesma, R.M., Rodríguez-Díaz, A.A., Estrada-Murillo, A.M., González-Romo, I.A., Magaña-Torres, E., 2019. Two new geothermal prospects in the Mexican Volcanic Belt: La Escalera and Agua Caliente-Tzitzio geothermal springs, Michoacán, México. *Geothermics* 80, 44–55. <https://doi.org/10.1016/j.geothermics.2019.02.004>.
- Jentsch, A., Jolie, E., Jones, D.G., Taylor-Curran, H., Peiffer, L., Zimmer, M., Lister, B., 2020. Magmatic volatiles to assess permeable volcano-tectonic structures in the Los Humeros geothermal field, Mexico. *J. Volcanol. Geotherm. Res.* 394, 106820. <https://doi.org/10.1016/j.jvolgeores.2020.106820>.
- Keeling, C.D., 1958. The concentration and isotopic abundances of atmospheric carbon dioxide in rural areas. *Geochim. Cosmochim. Acta* 13, pgs. 322–334. doi:[https://doi.org/10.1016/0016-7037\(58\)90033-4](https://doi.org/10.1016/0016-7037(58)90033-4).
- Kokh, M.A., Akinfiev, N.N., Pokrovskii, G.S., Salvi, S., Guillaume, D., 2017. The role of carbon dioxide in the transport and fractionation of metals by geological fluids. *Geochim. Cosmochim. Acta* 197, 433–466.
- Lan, X., Thoning, K.W., Dlugokencky, E.J., 2024. Trends in globally-averaged CH_4 , N_2O , and SF_6 determined from NOAA global monitoring laboratory measurements. Accessed on 2024-07. doi:[10.15138/P8XG-AA10](https://doi.org/10.15138/P8XG-AA10).
- Lanzafame, G., Tortorici, L., 1981. La tettonica recente della valle del fiume Crati. *Geogr. Fis. Din. Quat.* 4, 11–21.
- Li, C., Lu, Z., Ma, T., Zhu, X., 2009. A simple kriging method incorporating multiscale measurements in geochemical survey. *J. Geochem. Explor.* 101 (2), 147–154.
- Li, H., Meng, B., Yue, B., Gao, Q., Ma, Z., Zhang, W., Li, T., Yu, L., 2020. Seasonal CH_4 and CO_2 effluxes in a final covered landfill site in Beijing, China. *Sci. Total Environ.* 725, 138355. <https://doi.org/10.1016/j.scitotenv.2020.138355>.
- Liu, F., Zhou, X., Dong, J., Yan, Y., Tian, J., Li, J., Ouyang, S., He, M., Liu, K., Yoa, B., Wang, Y., Zeng, Z., Zhang, Y., 2023. Soil gas CO_2 emission from active faults: a case study from the Anninghe-Zemuhe fault, southeastern Tibetan plateau, China. *Front. Earth Sci.* 11, 1117862. <https://doi.org/10.3389/feart.2023.1117862>.
- Lombardi, S., Voltattorni, N., 2010. Rn, He and CO_2 soil-gas geochemistry for the study of active and inactive faults. *Appl. Geochem.* 25, 1206–1220. <https://doi.org/10.1016/j.apgeochem.2010.05.006>.
- Lyons, P.C., Alpern, B., 1989. Peat and coal: Origin, facies and depositional processes (Eds). In: *International Journal of Coal Geology* 12. Elsevier, Amsterdam.
- Ma, Y., Kong, X.Z., Zhang, C., Scheuermann, A., Brिंगemeier, D., Li, L., 2021. Quantification of natural CO_2 emission through faults and fracture zones in coal basin. *Geophys. Res. Lett.* 48 (7), e2021GL092693. <https://doi.org/10.1029/2021GL092693>.
- Ma, Y.Z., Zhang, X., 2019. *Quantitative Geosciences: Data Analytics, Geostatistics, Reservoir Characterization and Modeling*. Springer International Publishing, Cham, p. 640.
- Martikainen, P.J., Nykänen, H., Lang, K., Alm, J., Silvola, J., 1994. Emissions of methane and nitrous oxide from peatland ecosystems. In: Kanninen M., and Heikinheimo P., (Eds.): The Finnish research programme on climate change. Second progress report. Publications of the Academy of Finland 1/94: 279–284.
- Montzka, S.A. The NOAA annual greenhouse gas index (AGGI). NOAA global monitoring Laboratory, 2023. <https://gml.noaa.gov/aggi/aggi.html> (Accessed on 2024-07).
- Müller, D., Blum, A., Hart, A., Hooke, J., Kunkel, R., Scheidleder, A., Wendland, F., 2006. Final proposal for a methodology to set up groundwater threshold values in Europe. Deliverable D18, BRIDGE project, 63.
- National Oceanic and Atmospheric Administration, 2024. Carbon Cycle Greenhouse Gases in Global Monitoring Laboratory Retrieved October 23, 2024, from <https://gml.noaa.gov/ccgg/>.
- Neftel, A., Moor, E., Oeschger, H., Stauffer, B., 1985. Evidence from polar ice cores for the increase in atmospheric CO_2 in the past two centuries. *Nature* 315, 45–47. <https://doi.org/10.1038/315045a0>.
- Oertel, C., Matschullat, J., Zurba, K., Zimmerman, F., 2016. Greenhouse gas emission from soils-a review. *Geochem* 76, 327–352. <https://doi.org/10.1016/j.chemer.2016.04.002>.
- Pales, J.C., Keeling, C.D., 1965. The concentration of atmospheric carbon dioxide in Hawaii. *J. Geophys. Res.* 70(24), pgs. 6053–6076. doi:<https://doi.org/10.1029/JZ070i024p06053>.
- Panno, S.V., Kelly, W.R., Martinsek, A.T., Hackley, K.C., 2006. Estimating background and threshold nitrate concentrations using probability graphs. *Groundwater* 44 (5), 697–709. <https://doi.org/10.1111/j.1745-6584.2006.00240.x>.
- Pavelka, M., Acosta, M., Kiese, R., Altimir, N., Brümmer, C., Crill, P., Darenova, E., Fuß, R., Gielen, B., Graf, A., Klemetsson, L., Lohila, A., Longdoz, B., Lindroth, A., Nissim, M., Jiménez, S.M., Merbold, L., Montagnani, L., Peichl, M., Pihlatie, M., Pumpanen, J., Ortiz, P.S., Silvennoinen, H., Skiba, U., Vestin, P., Westin, P., Jonous, D., Kutsch, W., 2018. Standardisation of chamber technique for CO_2 , N_2O and CH_4 fluxes measurements from terrestrial ecosystem. *Int. Agrophys.* 32 (4), 569–587. <https://doi.org/10.1515/intag-2017-0045>.
- Pecoraino, G., Brusca, L., D'alessandro, W., Giannanco, S., Inguaggiato, S., Longo, M., 2005. Total CO_2 output from Ischia Island volcano (Italy). *Geochem. J.* 39 (5), 451–458. <https://doi.org/10.2343/geochemj.39.451>.
- Pérez-Zárate D., Santoyo E., Jácome-Paz M.P., Guevara M., Guerrero F.J., Yáñez-Dávila D., Santos-Raga G., 2024. Soil CO_2 fluxes measured in the Acozulco Geothermal System, Mexico: Baseline emissions from a long-term prospection programme. *Geochemistry, Volume 84, Issue 2, May 2024, 126112*. doi:<https://doi.org/10.1016/j.chemer.2024.126112>.
- Perri, F., Dominici, R., Guido, A., Cipriani, M., Cianflone, G., 2023. Geochemistry of mudrocks from the Calcare di base formation (Catanzaro Basin, Calabria): preliminary data. *Rend. Online Soc. Geol. Ital.* 59, 71–74. <https://doi.org/10.3301/ROL.2023.11>.
- Perri, F., Guido, A., Cipriani, M., Cianflone, G., Dominici, R., 2024. Geochemical and mineralogical proxies from the Messinian mudrocks (Catanzaro Basin, southern Italy): Paleoweathering and paleoclimate evolution during the onset of the Messinian salinity crisis. *Mar. Pet. Geol.* 163, 106703.
- Phuong, N.K., Harijoko, A., Itoi, R., Unoki, Y., 2012. Water geochemistry and soil gas survey at Ungaran geothermal field, Central Java, Indonesia. *J. Volcanol. Geotherm. Res.* 229, 23–33. <https://doi.org/10.1016/j.jvolgeores.2012.04.004>.
- Polemio, M., Luise, G., 2007. Conceptual and numerical model of groundwater flow for a coastal plain (Piana di Sibari, southern Italy). In proceedings of the XXXV IAH congress: groundwater and ecosystems, Lisbon, Portugal (pp. 17–21).
- PRIN, 2022. PNRR-thermal model of Aeolian Islands for new perspectives of sustainable exploitation of geothermal resources. CUP H53D23011420001.
- Raich, J.W., Schlesinger, W.H., 1992. The global carbon dioxide flux in soil respiration and its relationship to vegetation and climate. *Tellus B* 44 (2), 81–99.
- Raich, J.W., Tufekcioglu, A., 2000. Vegetation and soil respiration: correlations and controls. *Biogeochemistry* 48, 71–90.
- Randazzo, P., Caracausi, A., Aiuppa, A., Cardellini, C., Chiodini, G., Apollaro, C., Paternoster, M., Rosiello, A., Vespasiano, G., 2022. Active Degassing of Crustal CO_2 in Areas of Tectonic Collision: A Case Study from the Pollino and Calabria Sectors (Southern Italy). *Front. Earth Sci.* <https://doi.org/10.3389/feart.2022.946707>.
- Rella, C.W., Hoffnagle, J., He, Y., Tajima, S., 2015. Local- and regional-scale measurements of CH_4 , $\delta^{13}\text{C}\text{CH}_4$, and C_2H_6 in the Uintah Basin using a mobile stable isotope analyzer. *Atmos. Meas. Tech.* 8(10), pgs. 4539–4559. doi:<https://doi.org/10.5194/amt-8-4539-2015>.
- Saunio, M., Bousquet, P., Poulter, B., Peregón, A., Ciais, P., Canadell, J.G., Dlugokencky, E.J., Etiopie, G., Bastviken, D., Houweling, S., Janssens-Maenhout, G., Tubiello, F.N., Castaldi, S., Jackson, R.B., Alexe, M., Arora, V.K., Beerling, D.J., Bergamaschi, P., Blake, D.R., Brailsford, G., Brovkin, V., Bruhwiler, L., Crevoisier, C., Crill, P., Covey, K., Curry, C., Frankenberg, C., Gedney, N., Höglund-Isaksson, L., Ishizawa, M., Ito, A., Joos, F., Kim, H.-S., Kleinen, T., Krummel, P., Lamarque, J.-F., Langenfelds, R., Locatelli, R., Machida, T., Maksyutov, S., McDonald, K.C.,

- Marshall, J., Melton, J.R., Morino, I., Naik, V., O'Doherty, S., Parmentier, F.-J.W., Patra, P.K., Peng, C., Peng, S., Peters, G.P., Pison, I., Prigent, C., Prinn, R., Ramonet, M., Riley, W.J., Saito, M., Santini, M., Schroeder, R., Simpson, I.J., Spahni, R., Steele, P., Takizawa, A., Thornton, B.F., Tian, H., Tohjima, Y., Viovy, N., Voulgarakis, A., van Weele, M., van der Werf, G.R., Weiss, R., Wiedinmyer, C., Wilton, D.J., Wiltshire, A., Worthy, D., Wunch, D., Xu, X., Yoshida, Y., Zhang, B., Zhang, Z., Zhu, Q., 2016. The global methane budget 2000–2012. *Earth Syst. Sci. Data* 8, 697–751. <https://doi.org/10.5194/essd-8-697-2016>.
- Saunio, M., Bousquet, P., Poulter, B., Peregon, A., Ciais, P., Canadell, J.G., Dlugokencky, E.J., Etiope, G., Bastviken, D., Houweling, S., Janssens-Maenhout, G., Tubiello, F.N., Castaldi, S., Jackson, R.B., Alexe, M., Arora, V.K., Beerling, D.J., Bergamaschi, P., Blake, D.R., Brailsford, G., Bruhwiler, L., Crevoisier, C., Crill, P., Covey, K., Frankenberg, C., Gedney, N., Höglund-Isaksson, L., Ishizawa, M., Ito, A., Joos, F., Kim, H.-S., Kleinen, T., Krummel, P., Lamarque, J.-F., Langenfelds, R., Locatelli, R., Machida, T., Maksyutov, S., Melton, J.R., Morino, I., Naik, V., O'Doherty, S., Parmentier, F.-J.W., Patra, P.K., Peng, C., Peng, S., Peters, G.P., Pison, I., Prinn, R., Ramonet, M., Riley, W.J., Saito, M., Santini, M., Schroeder, R., Simpson, I.J., Spahni, R., Takizawa, A., Thornton, B.F., Tian, H., Tohjima, Y., Viovy, N., Voulgarakis, A., Weiss, R., Wilton, D.J., Wiltshire, A., Worthy, D., Wunch, D., Xu, X., Yoshida, Y., Zhang, B., Zhang, Z., Zhu, Q., 2017. Variability and quasi-decadal changes in the methane budget over the period 2000–2012. *Atmos. Chem. Phys.* 17, 11135–11161. <https://doi.org/10.5194/acp-17-11135-2017>.
- Saunio, M., Stavert, A.R., Poulter, B., Bousquet, P., Canadell, J.G., Jackson, R.B., Raymond, P.A., Dlugokencky, E.J., Houweling, S., Patra, P.K., Ciais, P., Arora, V.K., Bastviken, D., Bergamaschi, P., Blake, D.R., Brailsford, G., Bruhwiler, L., Carlson, K.M., Carrol, M., Castaldi, S., Chandra, N., Crevoisier, C., Crill, P.M., Covey, K., Curry, C.L., Etiope, G., Frankenberg, C., Gedney, N., Hegglin, M.I., Höglund-Isaksson, L., Hugelius, G., Ishizawa, M., Ito, A., Janssens-Maenhout, G., Jensen, K.M., Joos, F., Kleinen, T., Krummel, P.B., Langenfelds, R.L., Laruelle, G.G., Liu, L., Machida, T., Maksyutov, S., McDonald, K.C., McNorton, J., Miller, P.A., Melton, J.R., Morino, I., Müller, J., Murguía-Flores, F., Naik, V., Niwa, Y., Noce, S., O'Doherty, S., Parker, R.J., Peng, C., Peng, S., Peters, G.P., Prigent, C., Prinn, R., Ramonet, M., Regnier, P., Riley, W.J., Rosentreter, J.A., Segers, A., Simpson, I.J., Shi, H., Smith, S. J., Steele, L.P., Thornton, B.F., Tian, H., Tohjima, Y., Tubiello, F.N., Tsuruta, A., Viovy, N., Voulgarakis, A., Weber, T.S., van Weele, M., van der Werf, G.R., Weiss, R. F., Worthy, D., Wunch, D., Yin, Y., Yoshida, Y., Zhang, W., Zhang, Z., Zhao, Y., Zheng, B., Zhu, Q., Zhu, Q., Zhuang, Q., 2020. The global methane budget 2000–2017. *Earth Syst. Sci. Data* 12, 1561–1623. <https://doi.org/10.5194/essd-12-1561-2020>.
- Sbrana, A., Marianelli, P., Belgiojorno, M., Sbrana, M., Ciani, V., 2020. Natural CO₂ degassing in the mount Amiata volcanic-geothermal area. *J. Volcanol. Geotherm. Res.* 397, 106852. <https://doi.org/10.1016/j.jvolgeores.2020.106852>.
- Serrano-Silva, N., Sarría-Guzmán, Y., Dendooven, L., Luna-Guido, M., 2014. Methanogenesis and Methanotrophy in soil: a review. *Pedosphere* 24, 291–307. [https://doi.org/10.1016/S1002-0160\(14\)60016-3](https://doi.org/10.1016/S1002-0160(14)60016-3).
- Shaufler, G., Kizler, B., Schindlbacher, A., Skiba, U., Sutton, M.A., Zechmeister-Boltenstern, S., 2010. Greenhouse gas emission from European soil under different land use: effect of soil moisture and temperature. *Eur. J. Soil Sci.* 61, 683–696. <https://doi.org/10.1111/j.1365-2389.2010.01277.x>.
- Sinclair, A.J., 1974. Selection of threshold values in geochemical data using probability graphs. *J. Geochem. Explor.* 3 (2), 129–149. [https://doi.org/10.1016/0375-6742\(74\)90030-2](https://doi.org/10.1016/0375-6742(74)90030-2).
- Singh, A., Maichle, R., 2015. ProUCL Version 5.1 user guide. U.S. Environmental Protection Agency, Washington, DC. EPA/600/R-07/041. https://www.epa.gov/site/s/production/files/2016-05/documents/proucl_5.1_user_guide.pdf.
- Skeie, R.B., Hodnebrog, Ø., Myhre, G., 2023. Trends in atmospheric methane concentrations since 1990 were driven and modified by anthropogenic emissions. *Commun. Earth Environ.* 4, 317. <https://doi.org/10.1038/s43247-023-00969-1>.
- SNPA Gruppo di lavoro 9 bis, ISPRA, ARPA. Linea guida SNPA n.15/2018. Progettazione del monitoraggio di vapori nei siti contaminati - Appendice B - misure di flusso (flux chambers) in modalità attiva. https://www.snpambiente.it/wpcontent/uploads/2018/11/Appendice_B_linea_guida_snpa_15_2018.pdf.
- Tansi, C., Muto, F., Critelli, S., Iovine, G., 2007. Neogene-Quaternary strike-slip tectonics in the central Calabrian arc (southern Italy). *J. Geodyn.* 43 (3), 393–414. <https://doi.org/10.1016/j.jog.2006.10.006>.
- Tardani, D., Taussi, M., Robidoux, P., Sánchez-Alfaro, P., Pérez-Flores, P., Serrano, G., Morales, G., Tassara, S., Grassa, F., Soler, V., Morata, D., 2024. Gas geothermometry, soil CO₂ degassing, and heat release estimation to assess the geothermal potential of the Alpehue hydrothermal field (Sollipulli volcano, southern Chile). *Geothermics* 122, 103092. <https://doi.org/10.1016/j.geothermics.2024.103092>.
- Taussi, M., Nisi, B., Vaselli, O., Maza, S., Morata, D., Renzulli, A., 2021. Soil CO₂ flux and temperature from a new geothermal area in the Cordón de Inacaliri volcanic complex (northern Chile). *Geothermics* 89, 101961. <https://doi.org/10.1016/j.geothermics.2020.101961>.
- Taussi, M., Nisi, B., Brogi, A., Liotta, D., Zucchi, M., Venturi, S., Cabassi, J., Boschi, G., Ciliberti, M., Vaselli, O., 2023. Deep regional fluid pathways in an extensional setting: the role of transfer zones in the hot and cold degassing areas of the Larderello geothermal system (northern Apennines, Italy). *Geochim. Geophys. Geosyst.* 24, e2022GC010838. <https://doi.org/10.1029/2022GC010838>.
- Tazioli, G.S., 1986. *Indagini idrogeologiche volte allo sfruttamento delle risorse idriche sotterranee. Tecniche per la difesa dall'inquinamento, VII Corso di aggiornamento, Cosenza, Italy.*
- Tonani, F., Miele, G., 1991. Methods for measuring flow of carbon dioxide through soils in the volcanic setting. Napoli '91. International conference on active volcanoes and risk mitigation. Napoli. 27 August - 1 September 1991.
- Tregoures, A., Beneito, A., Berne, P., Gonze, M.A., Sabroux, J.C., Savanne, D., Burkhalter, R., 1999. Comparison of seven methods for measuring methane flux at a municipal solid waste landfill site. *Waste Manag. Res.* 17 (6), 453–458. <https://doi.org/10.1177/0734242X9901700608>.
- Van Dijk, J.P., Bello, M., Brancaleoni, G.P., Cantarella, G., Costa, V., Frixa, A., Golfetto, F., Merlini, S., Riva, M., Torricelli, S., Toscano, C., Zerilli, A., 2000. A regional structural model for the northern sector of the Calabrian arc (southern Italy). *Tectonophysics* 324, 267–320. [https://doi.org/10.1016/S0040-1951\(00\)00139-6](https://doi.org/10.1016/S0040-1951(00)00139-6).
- Vespasiano, G., Apollaro, C., Marini, L., Dominici, R., Cianflone, G., Romanazzi, A., Polemio, M., De Rosa, R., 2015a. Hydrogeological and isotopic study of the multi-aquifer system of the Sibari plain (Calabria, southern Italy). *Rend. Online Soc. Geol. Ital.* 38. <https://doi.org/10.3301/ROL.2015.158>.
- Vespasiano, G., Apollaro, C., Muto, F., De Rosa, R., Critelli, T., 2015b. Preliminary geochemical and geological characterization of the thermal site of Spezzano Albanese (Calabria, South Italy). *Rend. Online Soc. Geol. Ital.* 33, 108–110.
- Vespasiano, G., Apollaro, C., Muto, F., De Rosa, R., Dotsika, E., Marini, L., 2015c. Preliminary geochemical characterization of the warm waters of the Grotta delle Ninfe near Cerchiera di Calabria (South Italy). *Rend. Online Soc. Geol. Ital.* 39, 130–133.
- Vespasiano, G., Cianflone, G., Cannata, C.B., Apollaro, C., Dominici, R., De Rosa, R., 2016. Analysis of groundwater pollution in the Sant'Eufemia plain (Calabria—South Italy). *Ital. J. Eng. Geol. Environ.* 2, 5–15. <https://doi.org/10.4408/IJEGE.2016-02-0-01>.
- Vespasiano, G., Notaro, P., Cianflone, G., 2018. Water-mortar interaction in a tunnel located in the southern Calabria (southern Italy). *Environ. Eng. Geosci.* 24 (3), 305–315.
- Vespasiano, G., Cianflone, G., Romanazzi, A., Apollaro, C., Dominici, R., Polemio, M., De Rosa, R.A., 2019. Multidisciplinary approach for sustainable management of a complex coastal plain: the case of Sibari plain (southern Italy). *Mar. Pet. Geol.* 109, 740–759. <https://doi.org/10.1016/j.marpetgeo.2019.06.031>.
- Vespasiano, G., Marini, L., Muto, F., Auqué, L.F., Cipriani, M., De Rosa, R., Critelli, S., Gimeno, M.J., Blasco, M., Dotsika, E., Apollaro, C., 2021. Chemical, isotopic and geotectonic relations of the warm and cold waters of the Cotronei (Ponte Coniglio), Bruciarello and Repole thermal areas, (Calabria - southern Italy). *Geothermics* 96. <https://doi.org/10.1016/j.geothermics.2021.102228>.
- Vespasiano, G., Cianflone, G., Taussi, M., De Rosa, R., Dominici, R., Apollaro, C., 2023a. Shallow geothermal potential of the Sant'Eufemia plain (South Italy) for heating and cooling systems: an effective renewable solution in a climate-changing society. *Geosciences* 13 (4), 110. <https://doi.org/10.3390/geosciences13040110>.
- Vespasiano, G., Cianflone, G., Marini, L., De Rosa, R., Polemio, M., Walraevens, K., Vaselli, O., Pizzino, L., Cinti, D., Capecciacci, F., Barca, D., Dominici, R., Apollaro, C., 2023b. Hydrogeochemical and isotopic characterization of the Gioia Tauro coastal plain (Calabria-southern Italy): a multidisciplinary approach for a focused management of vulnerable strategic systems. *Sci. Total Environ.* 160694.
- Vespasiano, G., Marini, L., Muto, F., Auqué, L.F., De Rosa, R., Jimenez, J., Gimeno, M.J., Pizzino, L., Sciarra, A., Cianflone, G., Cipriani, M., Guido, A., Fuoco, I., Barca, D., Dotsika, E., Bloise, A., Apollaro, C., 2023c. A multidisciplinary geochemical approach to geothermal resource exploration: the Spezzano Albanese thermal system, southern Italy. *Mar. Pet. Geol.* 155. <https://doi.org/10.1016/J.Marpetgeo.2023.106407>. ISSN: 0264–8172.
- ViDEPI, *Visibilità Dati Esplorazione Petrolifera in Italia.* <http://unmig.sviluppoeconomico.gov.it/videpi/kml/webgis.asp>.
- Waddington, J.M., Day, S.M., 2007. Methane emissions from a peatland following restoration. *J. Geophys. Res. Biogeosci.* 112 (G3). <https://doi.org/10.1029/2007JG000400>.
- Werner, C., Cardellini, C., 2006. Comparison of carbon dioxide emissions with fluid upflow, chemistry, and geologic structures at the Rotorua geothermal system, New Zealand. *Geothermics* 35 (3), 221–238. <https://doi.org/10.1016/j.geothermics.2006.02.006>.
- Werner, C., Hurwitz, S., Evans, C., W., Lowerstern, J.B., Bergfeld, D., Heasler, H., Jaworowski, C., Hunt, A., 2008. Volatile emissions and gas geochemistry of hot spring basin, Yellowstone National Park, USA. *J. Volcanol. Geotherm. Res.* 178, 751–762. <https://doi.org/10.1016/j.jvolgeores.2008.09.016>.
- Werner, C.A., Hochstein, M.P., Bromley, C.J., 2004. CO₂-Flux of Steaming Ground at Karapiti, Wairakei. In: *Proceedings 26th NZ Geothermal Workshop.*
- Whalen, S.C., Reeburgh, W.S., 2000. Methane oxidation, production, and emission at contrasting sites in a boreal bog. *Geomicrobiol. J.* 17(3), pgs. 237–252. doi:<https://doi.org/10.1080/01490450050121198>.
- Yuce, G., Fu, C.C., D'Alessandro, W., Gulbay, A.H., Lai, C.W., Bellomo, S., Yang, T.Y., Italiano, F., Walia, V., 2017. Geochemical characteristic of soil radon and carbon dioxide within the dead sea fault and Karasu fault in the Amik Basin (Haratay), Turkey. *Chem. Geol.* 469, 129–146. <https://doi.org/10.1016/j.chemgeo.2017.01.003>.